This is a preprint draft. The published article can be found at: https://doi.org/10.1016/j.conbuildmat.2022.128648.

Please cite this paper as:

Al-Bashiti, M., Naser, M.Z. (2022). Verifying Domain Knowledge and Theories on Fire-induced Spalling of Concrete through eXplainable Artificial Intelligence. *Construction and Building Materials*. https://doi.org/10.1016/j.conbuildmat.2022.128648.

Verifying Knowledge Domain and Theories on Fire-induced Spalling of Concrete through eXplainable Artificial Intelligence

M. al-Bashiti[1], M.Z. Naser[1,2]
[1]School of Civil and Environmental Engineering & Earth Sciences (SCEEES), Clemson University, Clemson, SC 29634, USA
[2]AI Research Institute for Science and Engineering (AIRISE), Clemson University, Clemson, SC 29634, USA
E-mail: malbash@clemson.edu, E-mail: mznaser@clemson.edu, Website: www.mznaser.com

Abstract

This paper adopts eXplainable Artificial Intelligence (XAI) to identify the key factors influencing fire-induced spalling of concrete and to extract new insights into the phenomenon of spalling by investigating over 640 fire tests. In this pursuit, an XAI model was developed, validated, and then augmented with two explainability measures, namely, Shapley Additive exPlanations (SHAP) and Local eXplainable model-agnostic explanations (LIME). The proposed XAI model not only can predict the fire-induced spalling with high accuracy (i.e., > 92%) but can also articulate the reasoning behind its predictions (as in, the proposed model can specify the rationale for each prediction instance); thus, providing us with valuable insights into the factors, as well as relationships between these factors, leading to spalling. Our findings indicate that there are eight key factors that heavily govern spalling: 1) presence of Polypropylene fibers, 2) degree of moisture content, 3) heating rate, 4) maximum exposure temperature, 5) silica fume/binder ratio, 6) sand/binder ratio, 7) water/binder ratio and 8) fly ash/binder ratio. While these factors were also listed by the majority of the existing spalling theories, the contribution of each factor seems to vary significantly and, most importantly, was not quantified for the most part. Thus, the validated model was then utilized to contrast and quantify the spalling-based knowledge domain and theories as collected by some of the most cited studies in this domain.

Keywords: Spalling; eXplainable AI; Fire; Concrete.

1.0 Introduction

Concrete is an inert insulation building material, making it an attractive construction material from a fire engineering perspective. Yet, and regardless of its type, concrete has been shown to spall under fire conditions [1]. According to Khoury [2,3] normal strength concrete (NSC), high strength concrete (HSC), and ultra-high-performance concrete (UHPC) follow similar trends when heated, but the latter is more susceptible to spalling at elevated temperatures. Such spalling can cause acute and unpredictable damage to concrete structures.

The research area on the spalling front has witnessed a series of serious efforts aimed at overcoming the mystery of spalling and finding solutions to minimize or ultimately prevent the adverse effects of spalling. These efforts have accelerated with the rise of leaner constructions which often require modern concretes [4]. Thus, understanding the underlying mechanisms behind this phenomenon is critical as this allows us to better predict spalling, as well as arrive at possible solutions to minimize its adverse effects [5–7].

A look into the existing literature shows that spalling can occur due to 1) pore pressure accumulation as induced by the rise in temperature and evaporating moisture, 2) the presence of

compression forces upon heated surfaces as a result of thermal gradients, 3) the initiation of internal cracking due to difference in thermal expansion between aggregate and cement paste and/or thermal expansion/deformation between concrete and reinforcement bars, 4) and strength loss due to chemical transformations during heating [2,3,8].

To further elaborate on the above, there are a few common factors that influence spalling. For example, it is widely recognized that the degree of moisture content of concrete is a critical factor that can influence spalling, especially for mixtures containing more than 2–3% moisture content by weight [2,9]. The heating rate is another critical factor that is tied to spalling (i.e., spalling was detected under both high heating (above 10ºC/min) [10–12] and low heating rates (0.5-2ºC/min) [13,14]. In parallel to the heating rate, the maximum exposure temperature was also seen to influence spalling (with high temperatures exceeding 500-600ºC can increase spalling risk). The presence of silica fume in concrete mixtures also increases the risk of spalling [2,15–18]. In contrast, the inclusion of Polypropylene (PP) fibers has been noted to be an effective filler to reduce spalling [2,18–20] (with some exceptions [2]).

At the moment, structural fire engineers struggle to accurately predict the spalling phenomenon. So far, a few theories have been proposed to explain the effects of heat on concrete. The majority of such theories were arrived at from experimental tests and empirical analysis. However, little consensus has been reached on the fire-induced concrete spalling mechanisms [5,21]. This can be perceived as an opportunity to explore new approaches. The role of artificial intelligence (AI) can be an attractive choice given its rise within our domain [18], as it has not been heavily explored as much as fire testing and modeling methods [22].

Despite their proven merit in exploring structural fire engineering problems, AI models often comprise complex algorithms (hence, the perception of black-box models [23]). A common notion within such models is that they seem to be capable of predicting fire engineering phenomena with ease (and a high degree of accuracy). However, such models may not adequately describe the reasoning behind their accurate predictions [23,24]. In order to understand such reasoning, we need an additional method/technique to be able to dive into the black box and uncover how the model works well. Put another way, we ought to know why do AI models predict a given phenomenon accurately, and if we could understand the rationale behind such accurate predictions, then we may be able to extract new knowledge on the phenomenon at hand.

Thus, building an XAI model is crucial at this point to diagnose the reasoning behind such predictions [25]. Creating explainable models is also elemental to enable transparency between engineers and AI models [26–28]; since the end-users are likely to prefer and adopt interpretable solutions.

This work aims to maximize the positive potential of XAI for three objectives; 1) to create a model that can predict the spalling phenomenon accurately, 2) to extract new insights into fire-induced spalling as obtained by two explainability measures (SHAP and LIME), and 3) verify findings of notable studies against that of those attained from XAI by examining one of the largest databases on fire-induced spalling compiled so far (>640 tests). Finally, structural fire engineers will be able

to apply and extend upon our verified model with the help of the proposed XAI model, which will be provided at the end of this paper.

2.0 A brief overview of spalling theories and mechanisms:

Various studies have been conducted on the fire-induced spalling of concrete. One of the earliest systematic spalling tests conducted in the twentieth century was carried out by Gary [29–31] as reported by Mayer-Ottens [6,32]. These studies classified spalling into four general categories, 1) *aggregate spalling,* which is attributed to the mineralogical characters of the aggregates, 2) *surface spalling* that occurs at the surfaces of the structural elements, 3) *corner spalling*, which is an explosive spalling that takes place at the corners of members, and 4) *wall explosive spalling*, which is an explosive spalling that takes place in walls [6].

In parallel to the above classes of spalling, the open literature also classifies spalling according to three mechanisms, 1) *thermo-chemical*, 2) *thermo-hygral*, and 3) *thermo-mechanical*. There are two types of thermo-chemical spalling: sloughing-off spalling and post-cooling spalling, and both are primarily related to the decomposition of hydrated products and calcite and rehydration of calcium oxide. Thermo-hygral spalling is the type of spalling that occurs due to moisture clogging and pore pressure. And thermo-mechanical spalling is related to loading, stresses, and restraint conditions [5]. These three mechanisms are further articulated below.

Thermo-chemical spalling occurs when concrete is exposed to high temperatures and triggering a series of chemical reactions. For example, in the range of 25ºC to 100ºC, aggregates and the paste start to expand. At 150ºC, most of the water content in the concrete starts to evaporate, and the paste shrinks in return (while the aggregates keep expanding). As a result of these conflicting actions, micro-cracks are created. While concrete is hot and expansive, these microcracks are small, and once concrete cools down and shrinks, the cracks become larger. When the concrete loses strength during heating, the cracks further expand and open. Around 450ºC, the aggregates start to deteriorate, and hydration products, calcium hydroxide, and calcium silicate hydrate, also begin to decompose.

Such deterioration is heavily influenced by the type of aggregate used in the concrete mixture [2,5]. For example, flint aggregates (below 350ºC) and granite and quartz (up to 600ºC) aggregates undergo the above critical transformation. This makes granite and quartz a better choice to resist spalling[1] [26]. Overall, spalling is more likely to occur when lightweight aggregate is used. This is mainly because the lightweight aggregate contains a higher degree of free moisture, which causes the development of larger pore pressure inside the fire-exposed concrete member. Reaching about 550ºC to 600ºC, concrete starts to rapidly lose strength, which further accelerates the domino effects of the above reactions [2].

Thermo-hygral spalling is induced by moisture clogging and pore pressure build-up inside heated concrete. Under this mechanism, a layer of material saturated with water is formed, called a moisture clog zone [5,6,33]. When concrete heats, the available moisture is released outwards, while most of the moisture does travel towards the center of the concrete member until the

[1] During rapidly developing fires both granite and quartz can cause intense spalling of concrete.

thermodynamic conditions are satisfied for vapor condensation. In the core, the water starts to condense, and concrete resists the infiltration *permeation* of this water. When the vapor pressure exceeds the tensile strength of the concrete mix, the surface of the concrete spalls, thus exposing the internal layers to fire. This type of spalling is violent as it results as it is accompanied by energy released in the form of popping off of the pieces and small slices with a certain speed and a popping or cracking sound.

Thermo-mechanical spalling occurs when a concrete member is experiencing a fire, introducing thermal stresses generated from differential thermal gradients and thermal restraints inside the concrete member, which causes the concrete surface to experience triaxial stresses [34]. Note that the behavior of concrete under fire is a combination of all three mechanisms. Identifying and understanding their contributed factors is essential to understanding the spalling mechanism [5,34,35]. In this work, we will be focusing on the factors that contribute to the first two mechanisms.

Hasenjager [6,36] noted that, in general, fire-induced spalling is highly influenced by 1) heating rate, 2) sudden changes in member size and the volume of the aggregate used in the concrete mix, 3) water vapor pressure and gasses from the aggregate and the cement paste, as well as 4) exceeding the tensile strength by unilateral strain. According to Kang [5], thermo-chemical spalling is influenced by the decomposition of hydrated products and calcite and the rehydration of calcium oxide. It typically occurs at temperatures greater than 700°C.

Kang [5] also suggests that the thermo-hygral spalling is related to moisture content and moisture clogging phenomena, which occur when pressure exceeds the tensile strength of concrete. Hertz [37] pointed out that the moisture content in concrete must be considered the most critical factor in influencing explosive spalling. Hertz argued that NSC would not spall if it is dry. All other factors mentioned in this paper and other papers may contribute to the effect of spalling but cannot cause spalling without moisture and concluded that significant spalling is not expected when the moisture content is less than 3% by weight. However, the spalling effect can be mild when the moisture content is between 3-4% [37].

Eurocode states that spalling is unlikely to take place when the moisture content of concrete is lower than 3%. Not only but also, Khoury [2], Kodur [38], and Copier [39] concluded that high moisture content is a critical factor for explosive spalling, along with many other studies [40–42]. Also, a recent study by Klingsch [43] notes that even low moisture content can cause explosive spalling and confirms that the release of high pore pressure is more important than the initial moisture content in the concrete mix.

It is worth noting that discussions on moisture content and permeability date back to Harmathy [51], indicating that the lower the permeability of concrete, the higher the spalling risk is. This is also shown by Zhukov [52], who finds that granite-based concrete of 40MPa experienced spalling at 3% moisture by weight while 20MPa concrete experienced spalling at 4%. It should be noted that Eurocode [44] did not mention specifications regarding the permeability of concrete, which is widely agreed that is directly proportional to the migration of moisture content in a concrete member [2,4,40,45–47], not the tensile strength [48–50].

Hertz [54] noticed the high risk of spalling in concrete densified by silica fume (densified by means of ultra-fine particles smaller than the cement particles). According to Kang [5] and Klingsch [43], concrete with silica fume had a higher risk of thermal spalling than concrete without silica fume. Kodur [48] has also shown that concrete with silica fume densifies the pore structure and decreases permeability [48]. Kodur [38], while conducting experiments with the National Research Council of Canada(NRCC) and taking into consideration other laboratories' outcomes, reported that the permeability of concrete significantly influences spalling.

Typically, the probability of spalling under a high heating rate is more significant than when the member is experiencing a low heating rate. Khoury [2] suggested that heating rates above 3°C/min are critical rates [2]. However, spalling has also been observed for some dense concretes, which would never occur in traditional concrete. For UHPC with low permeability, spalling has been observed under both low and high heating rates [5].

Maximum exposure temperature is widely known to be a critical factor in fire-induced spalling. Kodur [38,48], Kang [5] and Khoury [2] proposed that the critical temperature for spalling is around 550°C with some exceptions[2] for Kang, specifying that the critical range is between 380-700°C for the different spalling mechanisms mentioned above. At the same time, Hertz[37] concluded that spalling often occurs near the critical point of steam at 374°C.

Khoury [2] reported that aggregates with rugged surfaces could increase the physical bonding with the cement paste and can mitigate spalling. In addition, Klingsch [43] stated that aggregates with low thermal expansion have more thermal compatibility with cement paste and can mitigate spalling. Barret [53] stated that the aggregate type influences spalling of concrete. Also, Kang [5] reported a similar conclusion and added that using flint as an aggregate of concrete induces aggregate spalling. Kodur [38] pointed out that using siliceous aggregate (i.e., quartz) in an HSC mix can increase the susceptibility of spalling compared to carbonate aggregate due to the high heating capacity of the carbonate aggregate (I.e., limestone). Kodur [38] also added that spalling would have a higher likelihood of occurring when the lightweight aggregate is used in the HSC mix, explaining that lightweight aggregates contain more free moisture than normal-weight aggregates.

There are a few solutions to mitigate spalling; one solution is by including PP fibers in the concrete mixture at about 2% by volume [38]. Those fibers start to melt at 170°C, which creates a network of relief channels for water vapor to escape and the pressure to be released [33]. It should be noted that ACI 216.1 [55], Jansson [1], Khoury [56], Kodur [38,57], Hertz [37], and many more demonstrated that using PP fibers in the HSC and UHSC mixtures could minimize the spalling effects[58,59]. Also, Klingsch [43] suggested that the use of PP fibers minimizes the risk of explosive spalling and reduces the amount of concrete spalled from the specimen (flaking).

According to Hertz [37] and Kodur [38,57], including steel fibers increases the tensile strength of concrete members, even at elevated temperatures, which will help to resist the pore pressure

[2] Kang is proposing different spalling mechanisms with different temperatures, which will be discussed later in this work.

generated from the heating moisture content or water inside the concrete. Under these circumstances, 2-3 hours are provided for the structure to resist fire without significant spalling, which will give enough time for evacuation proposes and firefighters to control the fire.

As one can see, the above notable studies have provided general guidance on the phenomenon of fire-induced spalling. However, much of the existing works on spalling were, understandably, limited by the testing scale or magnitude and/or span of explored factors [37,57,60,61]. We aim to further extend these studies by means of XAI.

3.0 Model description

This section describes the dataset used in developing the XAI model and the approach adopted in this study.

3.1 Dataset statistical details

The used dataset contained 646 test samples collected by Ref. [62–66]. This dataset comprises 16 independent variables known to influence fire-induced spalling in concrete and one dependent variable, which describes the occurrence of spalling via two labels: *no spalling* or *spalling*. The 16 independent variables are: water/binder ratio (%), aggregate/binder ratio (%), sand/binder ratio (%), heating rate (^{o}C/min), moisture content, maximum exposure temperature (^{o}C), silica fume/binder ratio (%), aggregate size (mm), GGBS/binder ratio (%), FA/binder ratio (%), PP fibers quantity (kg/m^3), PP fibers diameter (um), PP fibers length (mm), steel fibers quantity (kg/m^3), steel fibers diameter (mm), steel fibers length (mm). It should be noted that raw proportions were kept as a ratio of the binder for simplicity and consistency. The graphical distribution of all the variables in this dataset is plotted in Fig 1, and the statistical analysis that summarizes the collected dataset's main attributes is tabulated in Table 1.

This is a preprint draft. The published article can be found at: https://doi.org/10.1016/j.conbuildmat.2022.128648.

Please cite this paper as:

Al-Bashiti, M., Naser, M.Z. (2022). Verifying Domain Knowledge and Theories on Fire-induced Spalling of Concrete through eXplainable Artificial Intelligence. *Construction and Building Materials*. https://doi.org/10.1016/j.conbuildmat.2022.128648.

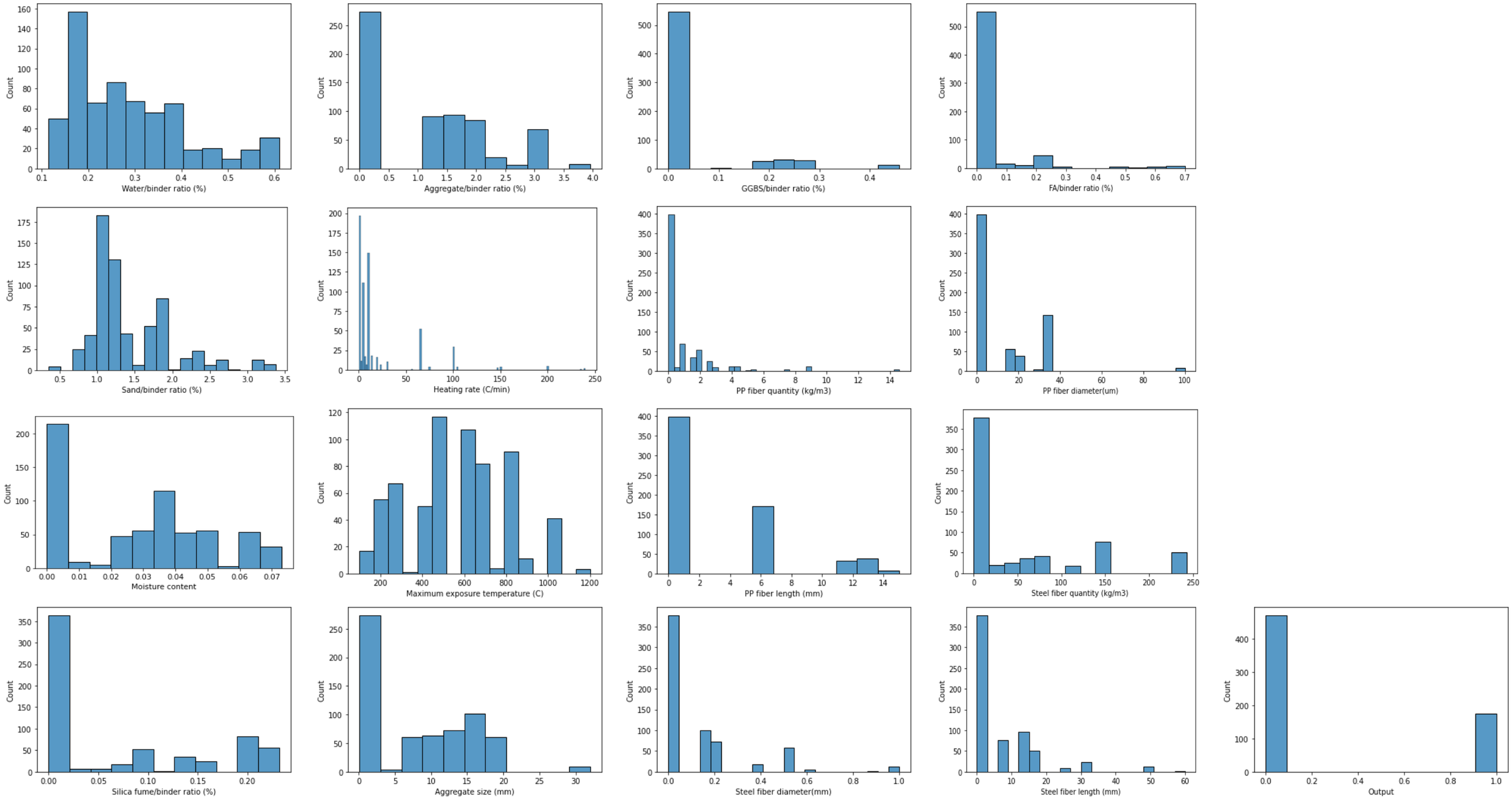

Fig. 1 Summary of statistical analysis of the fire-induced spalling concrete dataset.

This is a preprint draft. The published article can be found at: https://doi.org/10.1016/j.conbuildmat.2022.128648.

Please cite this paper as:

Al-Bashiti, M., Naser, M.Z. (2022). Verifying Domain Knowledge and Theories on Fire-induced Spalling of Concrete through eXplainable Artificial Intelligence. *Construction and Building Materials*. https://doi.org/10.1016/j.conbuildmat.2022.128648.

Table 1: Summary of statistical insights for the parameters of the dataset.

Parameter	Min	Max	Median	Mean	Standard deviation	Skew
Water/binder ratio (%)	0.12	0.61	0.27	0.29	0.12	0.93
Aggregate/binder ratio (%)	0.00	3.95	1.28	1.15	1.12	0.43
Sand/binder ratio (%)	0.35	3.38	1.22	1.40	0.55	1.34
Heating rate (°C/min)	0.25	240.00	7.00	20.85	36.93	2.93
Moisture content	0.00	0.07	0.03	0.03	0.02	0.13
Maximum exposure temperature (°C)	100.00	1200.00	600.00	561.28	234.32	0.13
Silica fume/binder ratio (%)	0.00	0.23	0.00	0.07	0.09	0.70
Aggregate size (mm)	0.12	32.00	8.00	8.26	7.60	0.52
GGBS/binder ratio (%)	0.00	0.46	0.00	0.04	0.10	2.54
FA/binder ratio (%)	0.00	0.70	0.00	0.04	0.11	3.73
PP fibers quantity (kg/m^3)	0.00	14.56	0.00	0.97	1.91	3.50
PP fibers diameter(um)	0.00	100.00	0.00	11.43	17.18	2.02
PP fibers length (mm)	0.00	15.00	0.00	3.12	4.43	1.15
Steel fibers quantity (kg/m^3)	0.00	243.00	0.00	51.48	76.76	1.35
Steel fibers diameter(mm)	0.00	1.00	0.00	0.13	0.21	2.11
Steel fibers length (mm)	0.00	60.00	0.00	6.30	10.25	2.38

In addition to the above statistical histograms and insights, the Pearson's correlation heatmap, which demonstrates the *linear* relationship between spalling and all other variables, can be seen in Fig. 2. This heatmap identifies which variables have the largest and lowest degrees of *linear* correlation with regard to spalling. In general, all parameters yielded a weak (i.e., 0.3-0.5) linear correlation to spalling. As such, we suspect the actual relationships are likely to be nonlinear. Despite the above, we report that the parameters with the largest *positive linear* correlation with spalling are maximum exposure temperature (0.42), moisture content (0.32), and heating rate (0.26), respectively. On the other side, the key factors that have a negative linear correlation to the occurrence of spalling are the PP fibers quantity (-0.18), followed by the water/binder ratio (-0.16), and then the sand/binder ratio (-0.15).

To overcome the linear assumption of the Pearson coefficient, the Spearman correlation coefficient, which measures the *monotonic* relation between a pair of variables, is listed in Fig. 2 too. From this lens, the parameters that positively influence the occurrence of spalling are maximum exposure temperature (0.69), moisture content (0.54), heating rate (0.46), and GGBS/binder ratio (0.42), arranged in descending order. On the other hand, the parameters that reduce the occurrence of spalling are the steel fibers length (-0.30) and diameter (-0.27), followed by the FA/binder ratio (-0.24).

A cross-examination of the Pearson and Spearman heatmaps shows that both maps are similar in terms of the parameters tied to the occurrence of spalling (i.e., maximum exposure temperature,

moisture content, and heating rate). However, they differ in terms of the parameters that seem to control spalling. This indicates that the factors governing fire-induced spalling of concrete are not linearly nor monotonically associated.

This is a preprint draft. The published article can be found at: https://doi.org/10.1016/j.conbuildmat.2022.128648.

Please cite this paper as:

Al-Bashiti, M., Naser, M.Z. (2022). Verifying Domain Knowledge and Theories on Fire-induced Spalling of Concrete through eXplainable Artificial Intelligence. *Construction and Building Materials*. https://doi.org/10.1016/j.conbuildmat.2022.128648.

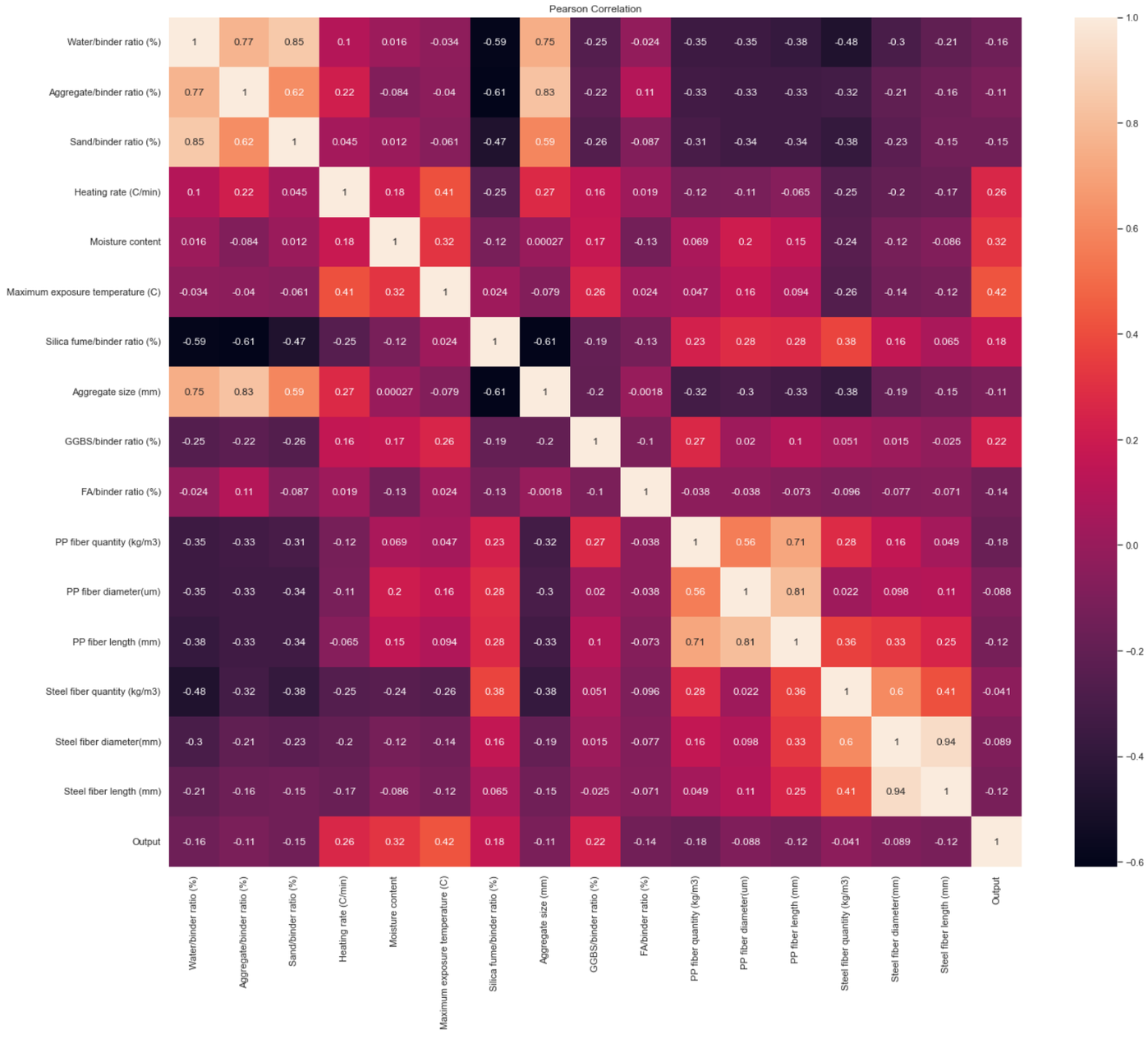

This is a preprint draft. The published article can be found at: https://doi.org/10.1016/j.conbuildmat.2022.128648.

Please cite this paper as:

Al-Bashiti, M., Naser, M.Z. (2022). Verifying Domain Knowledge and Theories on Fire-induced Spalling of Concrete through eXplainable Artificial Intelligence. *Construction and Building Materials*. https://doi.org/10.1016/j.conbuildmat.2022.128648.

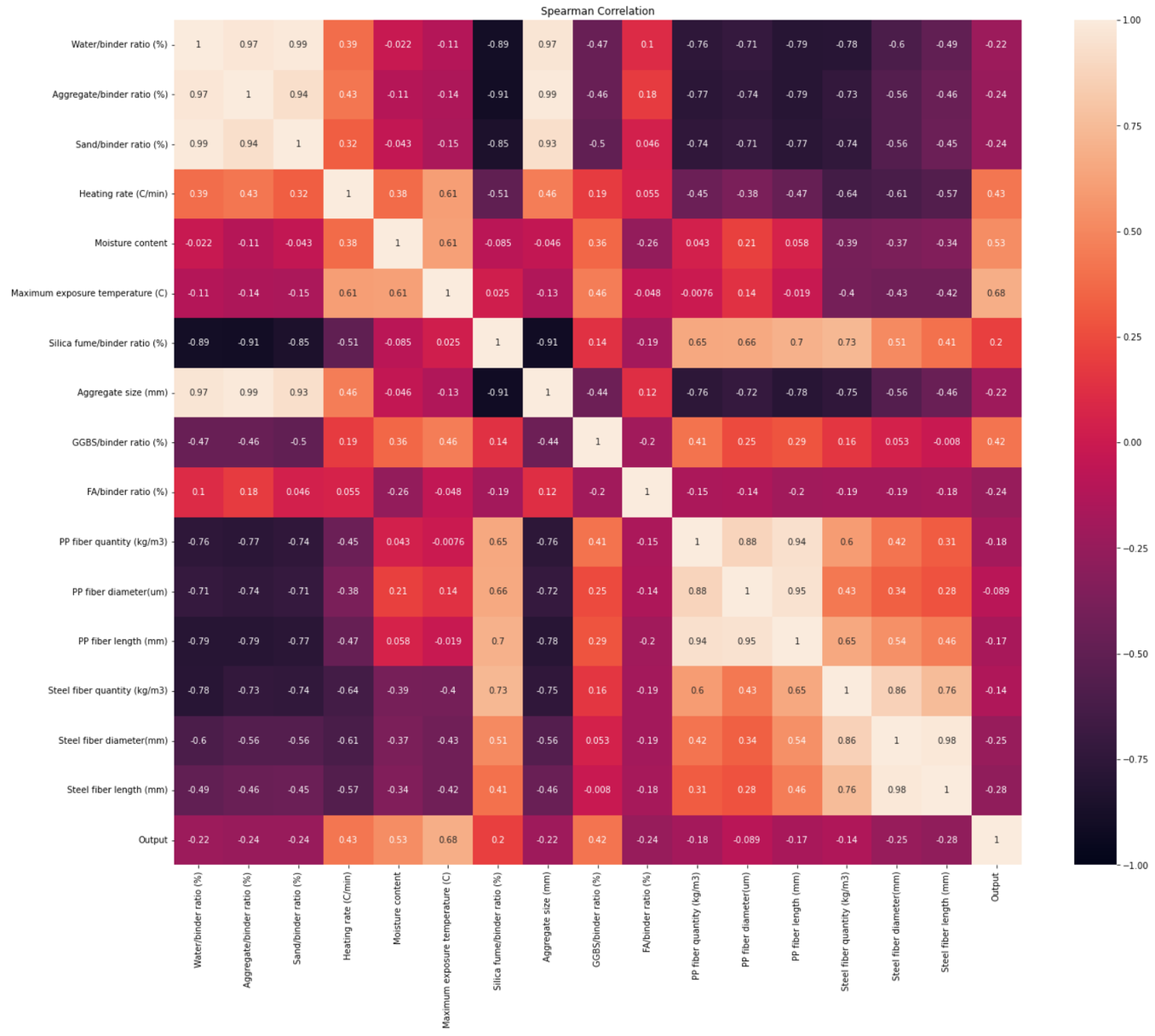

Fig. 2 Pearson correlation heatmap (top) and Spearman correlation heatmap (bottom)

This is a preprint draft. The published article can be found at: https://doi.org/10.1016/j.conbuildmat.2022.128648.

Please cite this paper as:

Al-Bashiti, M., Naser, M.Z. (2022). Verifying Domain Knowledge and Theories on Fire-induced Spalling of Concrete through eXplainable Artificial Intelligence. *Construction and Building Materials*. https://doi.org/10.1016/j.conbuildmat.2022.128648.

3.2 Details of the XGBoost algorithm

A supervised AI algorithm was used herein to build a model to accurately predict fire-induced spalling in concrete. We opt to use the XGBoost algorithm as a result of a recent study that we have recently published [67]. This is a decision-tree-based AI algorithm that uses a gradient boosting framework [68]. This algorithm assigns a numerical score to the tree leaves, and the score corresponds to whether the instance belongs to the decision. Once the tree reaches the end of the training data, the algorithm converts the numerical score into a categorical score leading to an answer for each instance. In our analysis, the developed algorithm was tweaked with the following settings: learning rate = *0.05*, objective = *binary: logistic*, missing value =*1*, seed = *42*, The degree of verbosity = *True*, early stopping rounds =*100*. The full code developed in this study will be provided in the Appendix.

The developed algorithm was trained and verified on the compiled dataset. The dataset was split into a *T*: training set, validated against the *V*: validation set, and independently tested against the *S*: testing set. In total, the *T* and *V* sets comprise 70% of the dataset, and the *S* set comprises 30%. Then, a *k*-fold cross-validation procedure is also applied. In such a procedure, the *T* set is randomly split up into k groups, wherein the model is trained using *k*-1 sets and then validated on the last *k* set. This procedure is repeated *k* times until each unique set has been used as the validation set. *k* in this study was taken as 10.

The performance of the model was then analyzed using dedicated classification performance metrics such as the *area under the (precision-recall) curve* (PR AUC) and the *confusion matrix*. The PR AUC displays the average of precision scores calculated for each recall threshold. Further, a confusion matrix was also used herein to examine the performance of the model. The confusion matrix showcases a visual comparison between the actual class and the predicted class. This matrix also homes other metrics such as sensitivity, precision, and accuracy (see Table 2). It is a table that represents the performance of the XGBoost classification algorithm and provides more insight into not only the performance of a predictive model but also which classes are being predicted correctly.

Table 2: Summary of evaluation metrics used in the AI model.

Performance metrics	Expression	Remarks
PR AUC	$AUC = \sum_{i=1}^{N-1} \frac{1}{2}(FP_{i+1} - FP_i)\,(TP_{i+1} - TP_i)$	*FP: number of false positives.* *TP: number of true positives.*
Confusion matrix	$Sensitivity\ (recall) = \frac{TP}{TP+FN}$ $Precision = \frac{TP}{TP+FP}$ $Accuracy = \frac{TP+TN}{TP+TN+FP+FN}$	*TN: number of true negatives),* *FN: number of false negatives*

This is a preprint draft. The published article can be found at: https://doi.org/10.1016/j.conbuildmat.2022.128648.

Please cite this paper as:

Al-Bashiti, M., Naser, M.Z. (2022). Verifying Domain Knowledge and Theories on Fire-induced Spalling of Concrete through eXplainable Artificial Intelligence. *Construction and Building Materials*. https://doi.org/10.1016/j.conbuildmat.2022.128648.

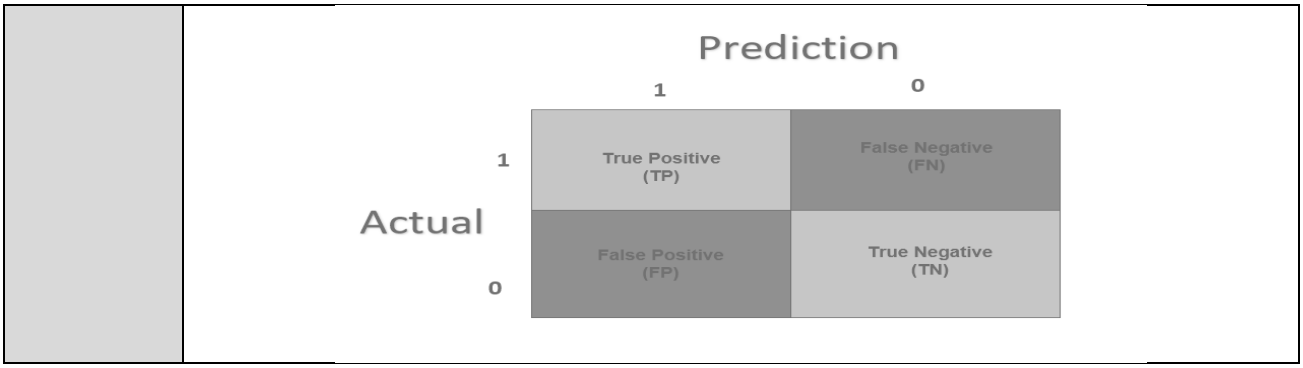

3.3 Explainability measures

The second objective of this work is to describe how the selected parameters of the compiled dataset in Table 1 contribute to spalling via two explainability measures, namely, SHAP and LIME.

Shapley Additive exPlanations (SHAP) [69] is an agnostic tool that can augment AI models by visualizing its output in terms of computing the contribution of each factor to the final prediction. Providing both *global* and *local* interpretation methods based on the aggregations of Shapley values instead of using factors in the dataset [70]. Mathematically expressed in Table 3, SHAP interpretations iterate over all possible factors and combinations of factors to ensure that the model accounts for the interactions between all individual factors. As one can see, the concept of SHAP is straightforward; however, when considering the interactions between the factors, this method can be timely and computationally intensive.

Table 3: Summary of explainability measures used in the XAI model.

SHAP	LIME
$\emptyset_i = \sum_{S \subseteq N \setminus \{i\}} \frac{\lvert S\rvert!(M-\lvert S\rvert-1)!}{M!} [f_x(S \cup \{i\}) - f_x(S)]$	$explanation(x) = \arg\min_{g \in G} L(f, g, \pi_x) = \Omega(g)$
S|!: the number of permutations of feature values that appear before *i*-th feature value. (|M|-|S|-1)! : represents the number of permutations of feature values that appear after the *i*-th feature value. The difference term in the above equation is the marginal contribution of adding the *i*-th feature value to S.	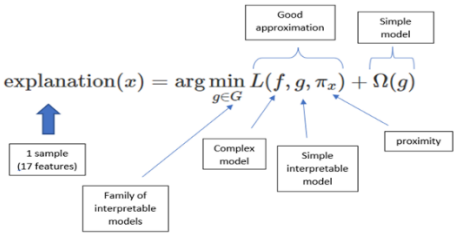

To get an overview (*global*) perspective and investigate the importance of each factor in the dataset, SHAP generates a feature importance graph *summary plot*. This plot uses the average

magnitude of Shapley values calculated using the equation provided in Table 3 and plots a series of horizontal graphs that represents the *contribution of each* factor. Overall, the graph sorts the factors in descending order from the highest contributor to the lowest based on their impact on the model prediction. On the local interpretability front, SHAP can also generate a *force plot* to represent the most critical factors influencing spalling and how each factor contributes to the prediction, starting from a *base value* (the averaged predicted probability across all samples).

In lieu of SHAP, LIME (Local eXplainable model-agnostic explanations) is another explainability measure. The basic idea of LIME is to zoom into each individual prediction, thus, providing *local* interpretability for the AI model. LIME works by modifying the input to the model *locally* instead of trying to understand the *entire model* simultaneously. A specific input instance is altered, and the impact on the predictions is monitored, which will help determine which changes will have the most impact on the prediction. The output of LIME is a list of illustrations reflecting the contribution of each factor to the prediction of a data sample [71].

LIME is also mathematically expressed in Table 3. The complex model is denoted with F, and the simple model 'local model' is denoted with g. This simple model g comes from a set of interpretable linear models denoted with G. The third argument, Pi, defines the local neighborhoods of that data point and is some sort of proximity measure. The second last term is used to regularize the complexity of our simple surrogate model. Ω is a complexity measure, and as this optimization problem is a minimization problem, we want to minimize the complexity.

4.0 Discussion and results

This section presents the findings and outcomes of our XAI analysis. This discussion starts by showcasing the validation of the XAI model, then presents the results of SHAP's explainability analysis (on the *global scale*: as in identifying the key factors that influence spalling and the interaction between these parameters taking into account the whole dataset) and then SHAP's and LIME's explainability analysis (on the *local scale*: as in identifying the model's rationale for individual predictions).

4.1 Model validation

As mentioned earlier, the PR AUC plot was used for the validation of the model. This graph illustrates the model's performance; the larger the area under the curve is, the better the model's accuracy. For example, a perfect AUC will be as far as it can from the dashed line, which indicates a general average performance. Note that as the curve gets closer to the upper left corner, the model's accuracy increases, indicating a higher accuracy model. Two AUC curves are illustrated in Fig. 3 to show the reader how accurate our model is in predicting spalling in the training and testing stages. The area under the curve was calculated using the *sklearn* library and turns out to be 90.7% for the training set and 86.6% for the testing set. Also, it can be seen that the true positives dominating the curve are as close to the upper left side as possible.

This is a preprint draft. The published article can be found at: https://doi.org/10.1016/j.conbuildmat.2022.128648.

Please cite this paper as:

Al-Bashiti, M., Naser, M.Z. (2022). Verifying Domain Knowledge and Theories on Fire-induced Spalling of Concrete through eXplainable Artificial Intelligence. *Construction and Building Materials*. https://doi.org/10.1016/j.conbuildmat.2022.128648.

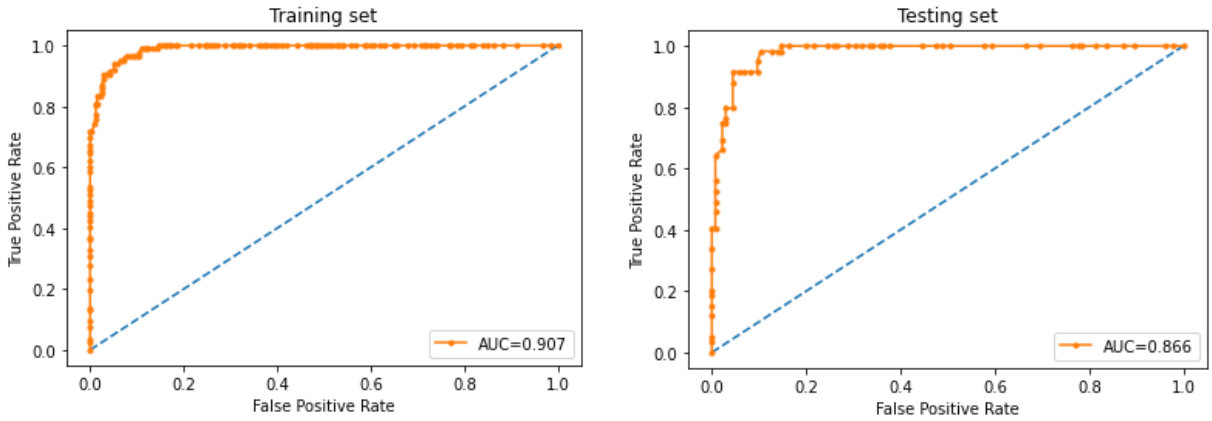

Fig. 3 Validation of model via the PR AUC metric

Figure 4 shows the confusion matrix used in this work to validate the developed model. This matrix shows exactly how many instances the model has correctly and mistakenly made. Both training set and testing sets achieved a good overall accuracy, precision and sensitivity. All the three evaluation metrics associated with the confusion matrix are tabulated together with the confusion matrix (see Fig. 4). It is clearly seen on the diagonal line from the top left to the bottom right that for the training set, 329 samples and 97 samples were correctly classified as no spalling, spalling, respectively. Similarly, 131 samples and 45 samples were correctly classified as spalling, spalling, respectively. In contrast, the model mis-performed in 26 (19+7) instances and 18 (14+4) instances during the training and testing stages, respectively.

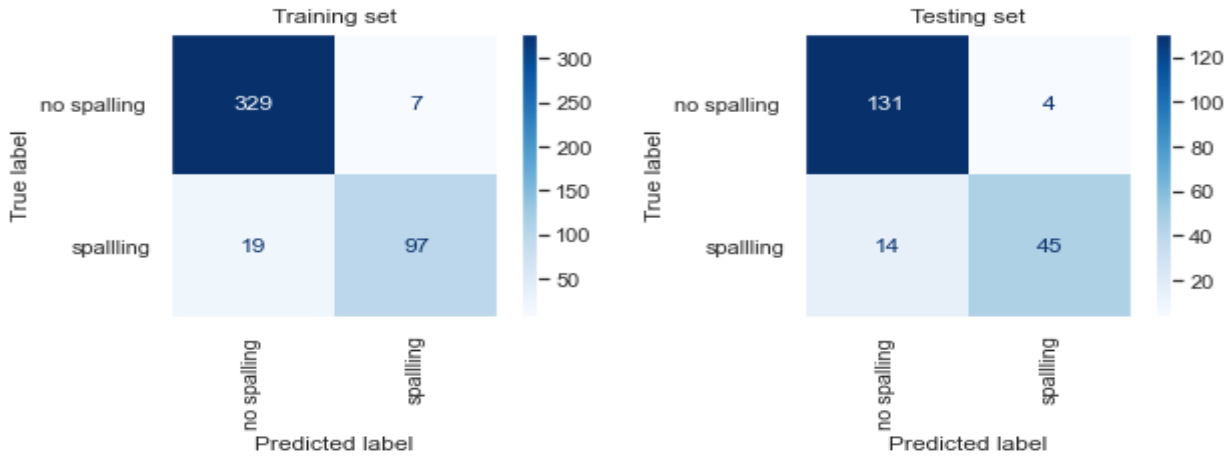

Class	Accuracy	Percision	Sensitivity
No Spalling	94%	95%	98%
Spalling		93%	84%

Class	Accuracy	Percision	Sensitivity
No Spalling	91%	90%	97%
Spalling		92%	76%

Fig. 4 Validation of model via the confusion matrix metric

This is a preprint draft. The published article can be found at: https://doi.org/10.1016/j.conbuildmat.2022.128648.

Please cite this paper as:

Al-Bashiti, M., Naser, M.Z. (2022). Verifying Domain Knowledge and Theories on Fire-induced Spalling of Concrete through eXplainable Artificial Intelligence. *Construction and Building Materials*. https://doi.org/10.1016/j.conbuildmat.2022.128648.

4.2 Global explainability

4.2.1 SHAP global plots

The explainability measure, SHAP, when augmenting the developed model, can generate two types of visualizations. Namely, the *Summary* plot and *factor importance* plot. These two visualizations will be covered herein.

The *Summary plot* represents the importance of each factor by reflecting the impact of each factor on the predictions' goodness. This plot orders the parameters vertically in terms of their importance to the model's accuracy (see Fig. 5). The same plot also demonstrates the range of points (e.g., feature value) each parameter has for that specific instance, so each point represents one sample associated with that particular parameter. Overall, one can see that parameters of large distributions seem to significantly affect the obtained predictions as opposed to parameters with narrower dispersion. In addition, this plot uses colors to distinguish the influence of the quantity of a given parameter upon the occurrence of spalling (i.e., red instances represent larger values and affect the model prediction depending on the side on which the red dots lie. For instance, a high quantity of PP fibers is likely to prevent spalling, while exposure to elevated temperatures increases the tendency to spalling.

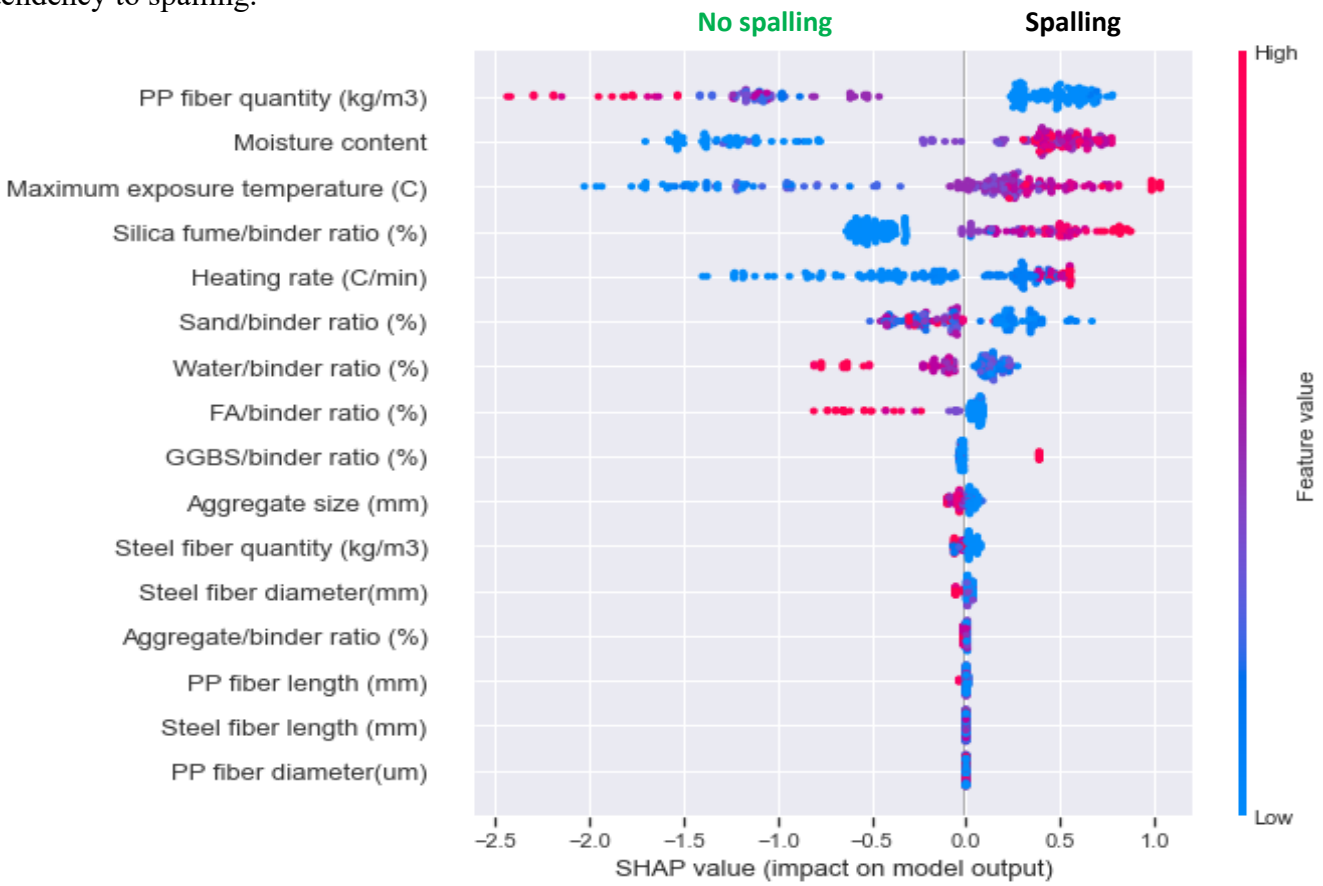

Fig. 5 Summary plot of SHAP values

353

354 A closer examination of Fig. 5 shows additional insights. For instance, the PP diameter is almost
355 at 0; not having a spread in either direction indicates that the factor does not seem to affect the
356 model's prediction. Similarly, by looking at the FA/binder ratio, the points are *skewed* to the
357 negative side, indicating a significant effect on the instances correctly predicted with no spalling
358 (i.e., *red color* dots represent that specimens with high values of FA/binder ratio did not spall as
359 much as their counterparts with low FA/binder ratio). On the other side, the spread can be
360 insignificant when the dots build over themselves (demonstrating that a high density of samples
361 having the same range of positive effects on the prediction). The blue-colored dots indicate that
362 specimens with lower FA/binder ratios are associated with *spalling*.

363 Similarly, the higher the PP fiber content, the lower the probability of spalling occurrence. It is
364 also clear that high values of any of the following factors: moisture content, maximum exposure
365 temperature, heating rate, and silica fume/binder ratio increase the likelihood of spalling. To
366 conclude, higher values of PP fibers and sand/binder, water/binder, FA/binder ratios mitigate
367 spalling. As opposed to having higher moisture content values, maximum exposure temperature,
368 silica fume/binder ratio, and heating rate influence the specimen positively to spall. The other
369 bottom eight parameters have an insignificant effect on the prediction.

370 In addition to the density *Summary plot* of SHAP, another visualization can be generated. This
371 new visualization is shown in Fig 6 and is referred to as the *factor importance plot*. The factor
372 importance plot lists the most significant parameters in descending order. The first listed
373 parameters contribute more to the model than the bottom ones (i.e., they have higher predictive
374 power than the lower ones). It should be noted that global importance gives an *average* overview
375 of all parameters and how they contribute to the model. However, Fig. 6 lacks the direction of
376 impact, e.g., whether a variable has a positive or negative influence.

377 Combining the outcomes of Figs. 5 and 6, one can see that eight parameters seem to heavily
378 influence the occurrence of spalling. These include PP fibers quantity, moisture content, maximum
379 exposure temperature, silica fume/binder ratio, heating rate, sand/binder ratio, water/binder ratio,
380 and FA/biner ratio. Thus, we will be focusing our discussion on these variables.

381

This is a preprint draft. The published article can be found at: https://doi.org/10.1016/j.conbuildmat.2022.128648.

Please cite this paper as:

Al-Bashiti, M., Naser, M.Z. (2022). Verifying Domain Knowledge and Theories on Fire-induced Spalling of Concrete through eXplainable Artificial Intelligence. *Construction and Building Materials*. https://doi.org/10.1016/j.conbuildmat.2022.128648.

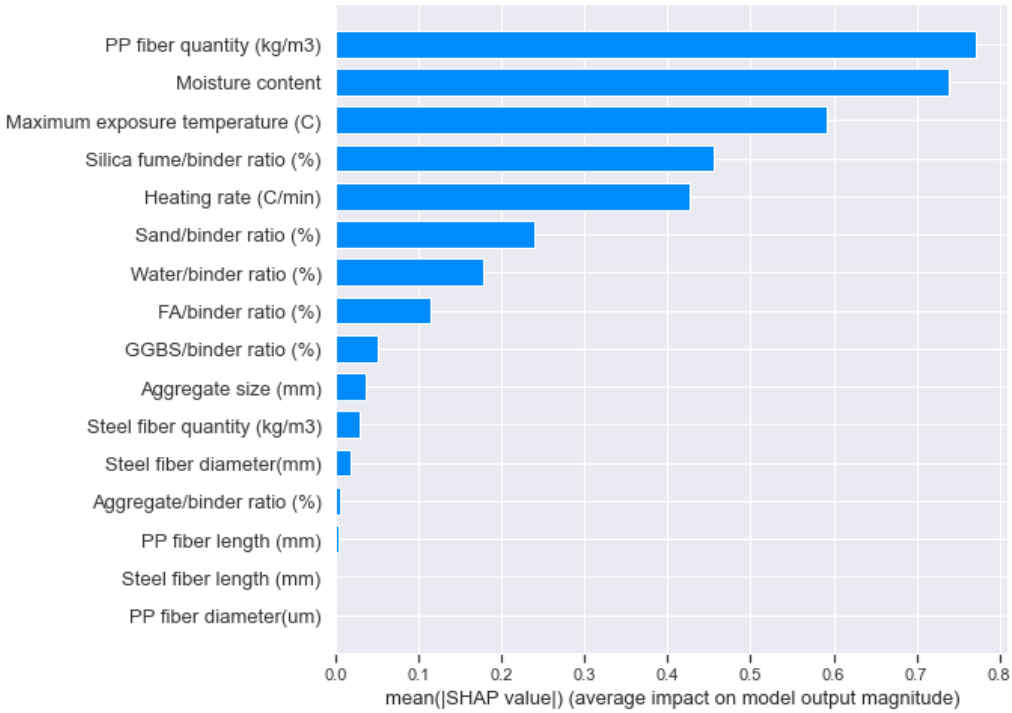

Fig. 6 Factor importance plot

4.2.2 Partial dependence plots

The Partial dependence plots are another model agnostic method that can be used for outlining the global explainability of XAI models. Such a plot depicts the relation between a specific parameter and the target variable (i.e., the occurrence of spalling/no spalling)[3]. The horizontal axis of this figure shows the value of the parameter on hand, and the vertical axis shows the probability of spalling occurrence (see Fig 7).

Looking at the *average*[4] of each partial dependence plot, one can see some critical trends. For example, the spalling tendency is tied to concrete mixtures with a moisture content that is larger than 3%. Similarly, the spalling tendency also increases when the exposure temperature increases beyond 400°C. In parallel, the risk of spalling seems to stabilize in the ranges of 200-500°C, 500-700°C, and beyond 700°C. We believe that this staggering trend could be due to the fire testing procedure followed in the sources used to compile the dataset, wherein these specific temperatures were explicitly used as maximum temperatures.

Further, the silica fume/binder ratio increase indicates a higher likelihood to spalling. The rise in heating rate (upward of 5°C/min) positively correlates with spalling; when the values increase, the

[3] Note that a partial dependence plot for a specific variable assumes that all other parameters remain unchanged (constant).

[4] We would like to point out that our discussion revolves around the average of the PDP to show the general observed trends as outcome from our analysis. The reader may also examine other individual trends as well.

likelihood of spalling occurrence also increases. The plot for PP quantity shows a unique response. This plot shows that using 0.5-0.75 kg/m^3 in the concrete mix can significantly decrease the probability of spalling; however, reaching a range of 0.8-0.9 kg/m^3 will increase the spalling occurrence to the same likelihood if the concrete mix did not include PP fibers. Finally, adding more than 1.0 kg/m^3 will decrease the spalling in the concrete mix again. At the moment, we are exploring the reasoning behind this unique response. We suspect that this can be attributed to some form of interaction between PP and other mix proportions. Overall, the inclusion of PP fibers > 2 kg/m^3 seems to significantly reduce the risk of spalling.

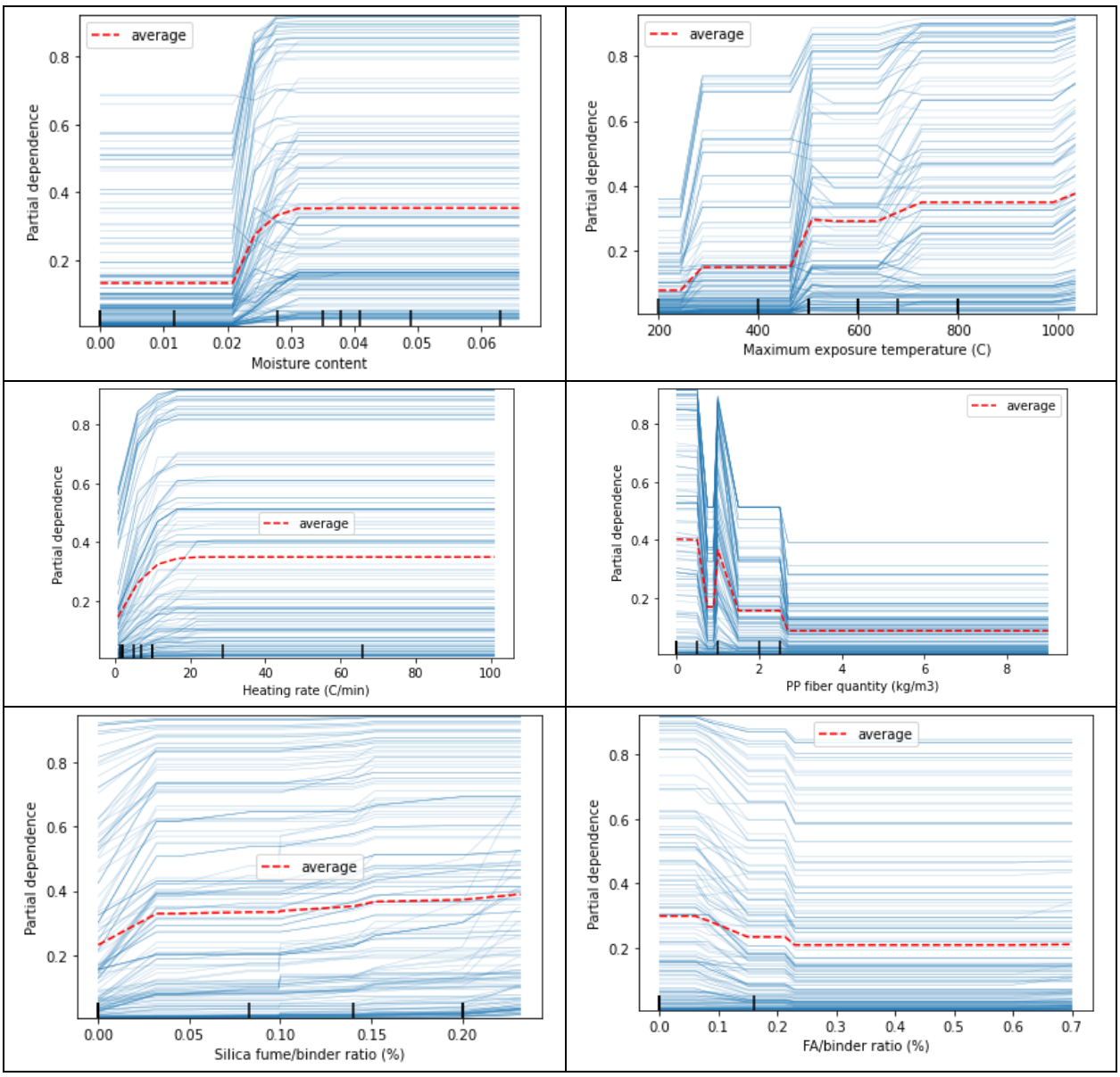

This is a preprint draft. The published article can be found at: https://doi.org/10.1016/j.conbuildmat.2022.128648.

Please cite this paper as:

Al-Bashiti, M., Naser, M.Z. (2022). Verifying Domain Knowledge and Theories on Fire-induced Spalling of Concrete through eXplainable Artificial Intelligence. *Construction and Building Materials*. https://doi.org/10.1016/j.conbuildmat.2022.128648.

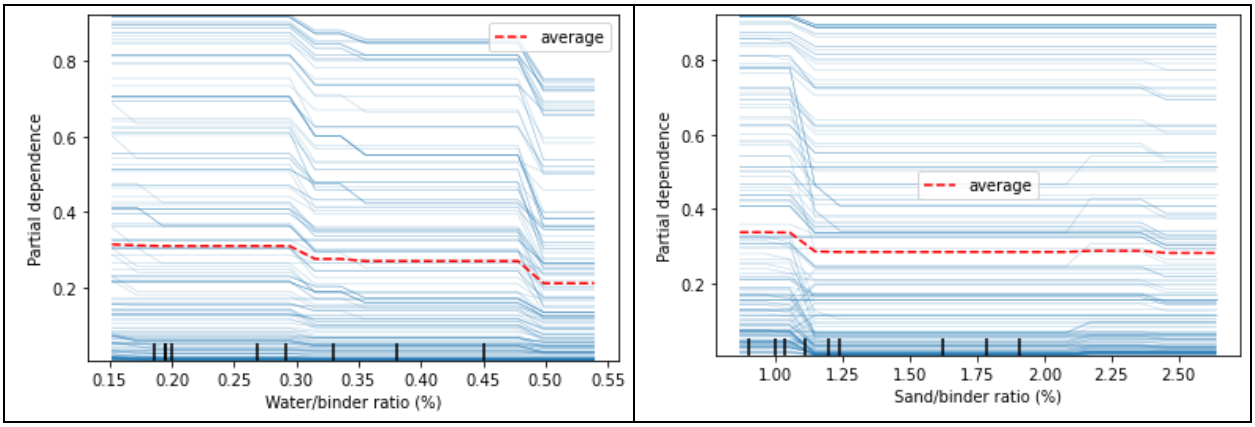

Fig. 7 Partial dependence plot for the top eight influencers of spalling

4.3 Local explainability

The previous section presents global explainability as obtained by SHAP from examining the model behavior (i.e., as averaged across all prediction cases). The same implies that the generated trends may differ (on average) between individual prediction instances.

Thus, this section will dive into showcasing local explainability for such individual cases to examine the model prediction for that instance by means of SHAP and LIME. For instance, Table 4 lists the concrete mixture for one sample used in the testing stage. This sample (which did not spall while being tested) will be examined via SHAP and LIME herein.

Table 4 Properties of a typical sample

Factor	Value	Factor	Value
Water/binder ratio (%)	0.269	FA/binder ratio (%)	0
Aggregate/binder ratio (%)	1.194	PP fibers quantity (kg/m^3)	0
Sand/binder ratio (%)	1.194	PP fibers diameter(um)	0
Heating rate (ºC/min)	2	PP fibers length (mm)	0
Moisture content	0	Steel fibers quantity (kg/m^3)	156
Maximum exposure temperature (ºC)	200	Steel fibers diameter(mm)	0.15
Silica fume/binder ratio (%)	0.099	Steel fibers length (mm)	6
Aggregate size (mm)	8		

4.3.1 SHAP local plot

The *Force* plot represents each parameter's contribution to the prediction for a specific observation (see Fig. 8). Another version of this plot is the waterfall plot (also see Fig. 8). The contribution of each parameter, starting with a calculated *SHAP base value* of 0.2363, adds up to the final prediction (i.e., with unity indicating spalling). In Fig 8, the larger the bar is, the higher the impact of its corresponding parameter on the predicted outcome. It allows the model to explain precisely how each prediction has been built up from all the individual factors in the model.

This is a preprint draft. The published article can be found at: https://doi.org/10.1016/j.conbuildmat.2022.128648.

Please cite this paper as:

Al-Bashiti, M., Naser, M.Z. (2022). Verifying Domain Knowledge and Theories on Fire-induced Spalling of Concrete through eXplainable Artificial Intelligence. *Construction and Building Materials*. https://doi.org/10.1016/j.conbuildmat.2022.128648.

Interpretation: The plot provides:

- The model predicted a low risk of spalling (meaning a *no spalling* occurrence).
- The base value: This would be predicted if there are no factors' values for the current output (base value: 0.2363 probability of spalling); it is simply the average of factors for all outcomes.
- The horizontal axis shows the contribution of each value to push the predicted value and *the impact of each factor on the prediction*.

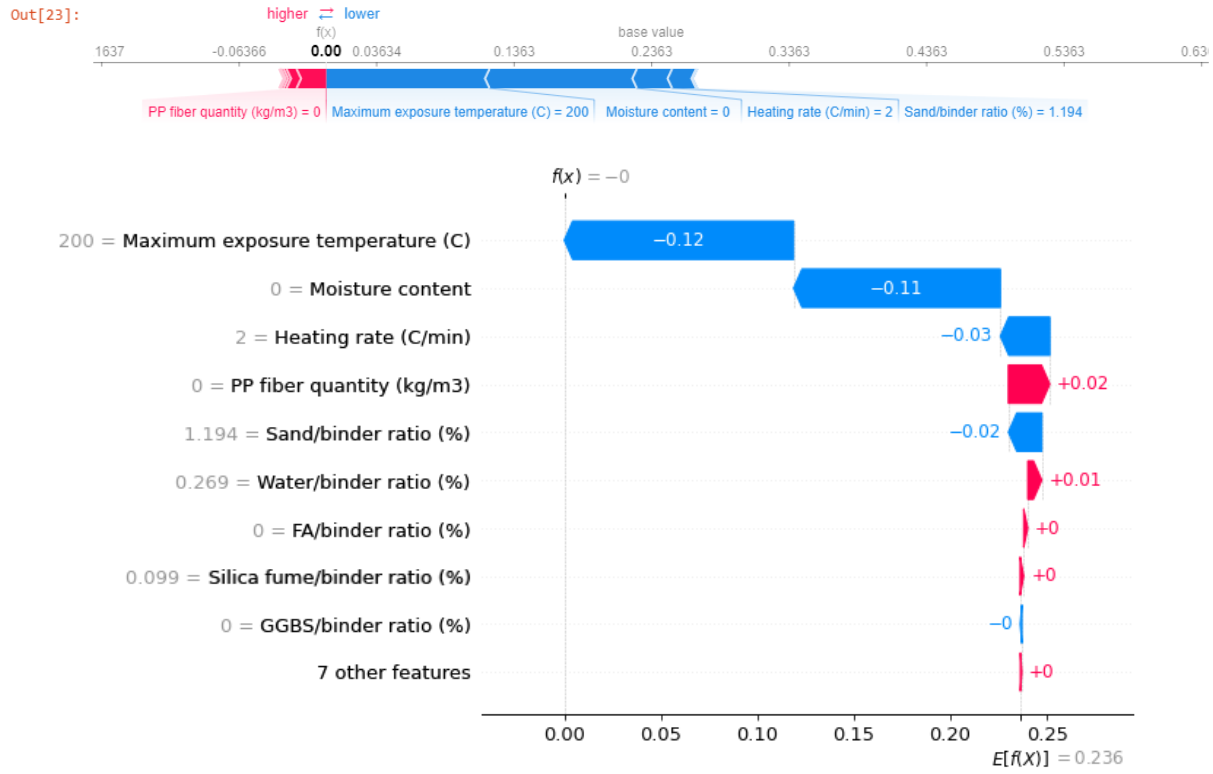

Fig. 8 Force plot (top) and water fall plot (bottom) of SHAP values for an individual instance

Figure 8 represents the top factors that significantly affect the model prediction for this specimen. For example, not including PP fibers in the concrete mix has led to considering the PP fibers as a positive influencer to spalling occurrence. On the opposite side, moisture content, maximum exposure temperature, and the heating rate decreased the prediction to be a non-spalling specimen. Note that for that instance, the maximum exposure temperature is less than the critical limit (500°C based on our analysis). A heating rate of 2°C/min is almost at the lower critical rate and seems to be a low rate, which pushes the prediction to a lower likelihood. Also, based on the analysis of this work (see Fig. 6), the moisture content is considered a direct influencer of spalling when it exceeds a limit of 2-3%. For this instance, moisture content = 0 (dry specimen) and hence further lowers the spalling effect.

This is a preprint draft. The published article can be found at: https://doi.org/10.1016/j.conbuildmat.2022.128648.

Please cite this paper as:

Al-Bashiti, M., Naser, M.Z. (2022). Verifying Domain Knowledge and Theories on Fire-induced Spalling of Concrete through eXplainable Artificial Intelligence. *Construction and Building Materials*. https://doi.org/10.1016/j.conbuildmat.2022.128648.

4.3.2 LIME local plot

The presented LIME method is applied to the same specimen examined above. To explain this result, the color indicator shows the variables positively associated with spalling in orange, and negatively correlated variables are shown in blue. In addition, the most significant variables affecting the prediction are listed in descending order. However, in local explainability, the order of those variables might change based on the different samples.

Interpretation: The LIME explainability table and chart show the following:

- The model predicted a value of 0.01 for spalling (meaning a 'non-spalling' occurrence).
- The vertical axis lists the contribution of each parameter to push the predicted value in descending order.
- Each parameter has two numbers associated with it. The first number shows the critical range related to the direction of the prediction, and the second shows the contribution of that parameter.

Comparing the XAI results of both SHAP, and LIME shows an identical response in classifying the specimen as spalling and no spalling.

Fig. 9 LIME interpretability visualization for an individual instance

Figure 9 shows the key factors that significantly affect the model prediction for the same instance as that examined via SHAP. Not including PP fibers in the concrete mix increases the likelihood of this specimen to spall. In contrast, moisture content, maximum exposure temperature, and the heating rate lowered the prediction to be a non-spalling specimen. Note, for that instance, the maximum exposure temperature is less than the critical limit of 500°C (as seen in Fig. 6). A heating rate of 2°C/min is on the low end as well as the fact that this is a dry specimen both pushed the prediction towards no spalling.

Comparing the XAI results of both SHAP and LIME was almost identical in classifying the specimens, which shows that building an AI model with different algorithms is a promising approach to understanding the spalling history of individual specimens. However, LIME and SHAP measures have shown slightly different key factors from a local point of view. Please refer to Appendix B for such comparisons between some of the examined specimens.

5.0 Comparison between existing spalling theories and XAI findings

This section compares the outcome of the presented XAI analysis against existing theories of fire-induced spalling of concrete. We view this as an exciting exercise since that much of the existing theories were not examined nor developed from large-scale testing (as opposed to the compiled 640+ tests here). This section also proposes possible recommendations to reduce the spalling tendency of concrete based on our findings as well as those reviewed from the open literature. Table 5 demonstrates the outcomes of the literature review of the most important papers on the fire-induced spalling of concrete.

A look into the parameters selected in the compiled database shows that these parameters can be grouped under *exogenous* factors (i.e., maximum exposure temperature and heating rate) and *endogenous* factors (such as moisture content, PP fibers quantity, etc.). It is clear that the exogenous parameters are related to fire and its effect on the heated surfaces. More importantly, these parameters were positively tied to the event of spalling.

This is a preprint draft. The published article can be found at: https://doi.org/10.1016/j.conbuildmat.2022.128648.

Please cite this paper as:

Al-Bashiti, M., Naser, M.Z. (2022). Verifying Domain Knowledge and Theories on Fire-induced Spalling of Concrete through eXplainable Artificial Intelligence. *Construction and Building Materials*. https://doi.org/10.1016/j.conbuildmat.2022.128648.

Table 5 Comparison between existing spalling theories and XAI findings

Factors	Kodur [38,72]	Kang [5]	Khoury [2,56]	Hertz [37]	Klingsch [43]	XAI
Moisture content	Higher moisture content levels lead to greater spalling.	The higher the moisture content, the greater the spalling risk.	> 3% is tied to spalling.	No spalling under 3%, mild spalling up to 4%	Low concrete permeability is the reason behind the spalling when the moisture content is presented.	Risk for spalling increases beyond 2%.
PP fibers	0.1 – 0.25 per volume.	The addition of *a certain amount* can prevent spalling even if it's under high heating rates	2 kg/m^3	The addition of PP fibers can be effective in mitigating spalling of dense concrete.	2 – 3 kg/m^3	Risk for spalling significantly reduces beyond 2.5 kg/m^3.
Maximum exposure temperature (ºC)	Positively influences spalling.	Thermo-mechanical: 430-660ºC, Thermo-chemical: 700-900ºC, Thermo-hygral: 220-320ºC.	550-600ºC.	Critical point of steam at 374ºC.	500ºC.	Risk for spalling increases beyond 500ºC.
Silica fume/binder ratio (%)	Unfavorable in a concrete mix.	Significant spalling for samples with high silica fume (at 0.15).	Unfavorable in a concrete mix.	Increases the probability of explosive spalling.	Silica fume increases the risk of explosive spalling significantly since it lowers the permeability of concrete	Risk for spalling increases beyond 0.03.
Heating rate (ºC/min)	The extent of spalling is much higher when the specimens are exposed to faster heating rates or higher fire intensities.	The chances are higher when heating rates are high, but if UHPC is used, spalling occurs even under low heating rates.	3ºC/min.	The rapid heating gives rise to large temperatures and moisture gradients in the fire-exposed parts.	Low heating rates could prevent explosive spalling, depending on the concrete mix.	Risk for spalling increases beyond 5ºC/min.
Aggregate type	Carbonate, normal-weight aggregates (limestone).	Preferably not flint.	Prefer rugged surfaces with low thermal expansion.	The effect is local near the stone and has, in general, no structural significance.	A lower thermal expansion is thought to reduce the risk of spalling due to a lower level of internal stresses.	-
Water/binder ratio (%)	-	-	Low water/cement ratio increases the risk of explosive spalling.	For super dense concrete, the crystal water can be sufficient for causing an explosive spalling.	High cement content influences spalling due to the increases of the total amount of water added to concrete, even at low water/cement ratios.	Low water/cement ratio increases the risk of spalling.
Cement	-	Limit the amount of cement/unit volume of concrete can mitigate the thermo-chemical	Calcium hydroxide is not desirable because it dissociates at about 400ºC.	-		-

The first *exogenous* factor is the maximum exposure temperature. For example, most of the XAI model outcomes were found to rely on the 500°C range to indicate the direction of the impact on the model prediction (i.e., for specimens exposed to temperatures that exceed this limit, the XAI model noted a trend in which such samples are more likely to spall). This tendency to spall falls as the maximum exposure temperature reduces. Based on Khoury's [2] findings, the critical temperature range of spalling is between 550-600°C. Also, Hertz [37] suggested that the critical point is around 374°C. Kang [5] indicated that thermo-hygral spalling occurs at a temperature range of 220-320°C, while the thermo-mechanical critical temperature is between 430-660°C, and thermo-chemical occurs at elevated temperatures above 700°C. It can be seen that different spalling types might happen at different temperatures; however, based on our analysis and Klingsch [43], the critical temperature is around 500°C, which is in the range of other theories.

The heating rate is the second exogenous parameter. Our findings suggested that a 5°C/min heating rate is a critical point that can positively influence spalling, where specimens exposed to a higher rate are much more likely to spall. This observation agrees with Khoury [2] and Kang [5]. In a more dedicated work, Cheo et al. [73] examined the effect of low and high heating rates: 1°C/min and 18°C/min and reported that specimens heated at a lower heating rate have a lower probability of spalling.

On the other hand, the *endogenous* factors relate to the mixture proportions, and as such, these are more likely to be controlled. The above brings an opportunity to explore possible means to control spalling. We will be focusing our comparison of endogenous parameters on 1) pp fibers quantity, 2) moisture content, 3) silica fume/binder ratio, 4) sand/binder ratio, 5) water/binder ratio, 6) FA/binder ratio.

PP fibers is considered the most critical *endogenous* factor in the XAI model. Both local and global XAI analyses suggest that adding PP fibers can significantly reduce the spalling occurrence. However, the partial dependence plot showed some fluctuation between the 0.75-0.9 kg/m^3 and a steady trend beyond 2.5 kg/m^3 which was pointed out earlier. Khoury [2,56], Kang [5], Hertz [37], Kodur [38], Klingsch [43], and Jansson [6] explained that the increment of PP fibers would increase the permeability of concrete, which will effectively mitigate spalling.

Many of the existing theories [34,35,37] show how crucial is the presence of moisture content to predict the spalling phenomena. Kang [5], Khoury [2], Kodur [38], and Copier [39], in parallel with the Eurocode [44], agree that the spalling of concrete is much more likely to occur when the moisture content exceeds 2-3% by weight of concrete. Also, our XAI analysis shows that a range of 2-3% is the critical range and the partial dependence plots show a sudden change in the direction between those limits. Comparing the theoretical and XAI model's outcomes seemed to match each other. This shows our model's accuracy and indicates how critical the moisture content is in predicting spalling.

The silica fume/binder ratio is also one of the most important factors in the model. XAI model predicts that the presence of the silica fume/binder ratio in the concrete mix would influence spalling; however, after looking at the partial dependence plot, we found that spalling is highly influenced beyond the range of 0-0.03. Also, both SHAP and LIME tools predicted that the presence of silica fume constantly pushed the prediction to be a spalling specimen with no specific value. Hertz [54], Kodur [72], Klingsch [43], Khoury [2], and Kang [5] concluded from the literature review that concrete mixtures with silica fume have low permeability, which explains the higher propensity for spalling.

Water- sand- and FA/binder ratios are critical factors significantly affecting the spalling predictions; using these parameters in a concrete mix will negatively influence the occurrence of spalling. XAI model shows that the critical limit of sand/binder ratio to include in a concrete mix is around 1.05-1.15, while for water/binder ratio, the range is slightly under 0.5. Also, FA binder/ratio is recommended by the partial dependence plots to be above 0.22. Around these ratios, spalling propensity is likely to decrease, such that higher ratios decrease the occurrence probability. Khoury [2] and Kodur [38] agree with this ratio's qualitative outcome.

From the outcomes of this paper and the XAI model, we recommend the following values fo the key parameters involved in concrete mix.

Table 6 Recommended values to minimize spalling.

Factor	Recommended value*
PP fibers quantity (kg/m^3)	> 2.5
Moisture content	< 2%
Silica fume/binder ratio (%)	0
Sand/binder ratio (%)	1.15
Water/binder ratio (%)	> 0.3
FA/binder ratio (%)	> 0.22

*For the full range, please re-visit Fig. 7.

6.0 Limitations and future work

We acknowledge the existence of other parameters than those examined which could have been tied to spalling (such as specimen size and configuration, loading level, heating duration, aggregate type, permeability and pore size, use of different fiber types such as PE or nylon, etc.). Admittedly, such factors were not examined in this study as our analysis primarily focused on parameters associated with raws often utilized in concrete mixtures as well as small concrete specimens (i.e., cubes and cylinders). We hope to be able to explore the influence of other factors and size effect in large load bearing members in a future work. We also invite the readers of this work to further expand our analysis (by leveraging the attached XAI Python code) and seek companion research directions to that presented in this study.

7.0 Conclusions

This paper presents a new perspective on fire-induced spalling in concrete by creating an XAI model. This model was validated and achieved > 92% accuracy. Then, the model was augmented with explainability measures (SHAP and LIME) to uncover new insights into the phenomenon of spalling. The main conclusions from our analysis are summarized as follows.

1. We identified two types of factors that can influence spalling, *exogenous* (i.e., maximum exposure temperature and heating rate) and *endogenous* factors (such as moisture content, PP fibers quantity, etc.).
2. The top positive influencers of fire-induced spalling are moisture content, maximum exposure temperature, silica fume/binder ratio, and heating rate.
3. The top negative influencers of fire-induced spalling are pp fibers quantity, sand/binder ratio, water/binder ratio, and FA/binder ratio.
4. The addition of PP fibers to the concrete mix can reduce spalling tendency (especially in mixtures of more than 2.5 kg/m^3).
5. Spalling is negatively proportional to the sand/binder ratio, water/binder ratio, and FA/binder ratio; when their presence increases, the spalling decreases.
6. The presence of silica fume/binder ratios increases the probability of spalling. Also, exposure to temperatures larger than 500ºC and/or heating rates larger than 5ºC/min increases spalling.
7. Moisture content is considered a key factor affecting the spalling of concrete. The critical range is between (2-3%) and is significantly influencing spalling of concrete.

This is a preprint draft. The published article can be found at: https://doi.org/10.1016/j.conbuildmat.2022.128648.

Please cite this paper as:

Al-Bashiti, M., Naser, M.Z. (2022). Verifying Domain Knowledge and Theories on Fire-induced Spalling of Concrete through eXplainable Artificial Intelligence. *Construction and Building Materials*. https://doi.org/10.1016/j.conbuildmat.2022.128648.

Appendix A

The proposed XAI model is provided herein.

```
from xgboost import XGBClassifier
import xgboost as xgb
import seaborn as sns
import pandas as pd
import numpy as np
from matplotlib import pyplot
from sklearn.model_selection import train_test_split
from sklearn.metrics import roc_curve
from sklearn.feature_selection import mutual_info_classif
from sklearn.metrics import confusion_matrix,classification_report
from sklearn.metrics import accuracy_score
from sklearn.metrics import balanced_accuracy_score, roc_auc_score, make_scorer
from sklearn.metrics import plot_confusion_matrix
from sklearn.model_selection import StratifiedKFold
from sklearn.model_selection import cross_val_score
```

In [2]:

```
fire=pd.read_csv('database.csv')

fire
```

Out[2]:

	Water/binder ratio (%)	Aggregate/binder ratio (%)	Sand/binder ratio (%)	Heating rate (C/min)	Moisture content	Maximum exposure temperature (C)	Silica fume/binder ratio (%)	Aggregate size (mm)	GGBS/binder ratio (%)	FA/binder ratio (%)	PP fiber quantity (kg/m3)	PP fiber diameter(um)	PP fiber length (mm)	Steel fiber quantity (kg/m3)	Steel fiber diameter(mm)	Steel fiber length (mm)	Output
0	0.273	2.000	1.049	101.0	0.049	1034	0.0	7.0	0.25	0.0	0.0	0.0	0	0.0	0.0	0	1
1	0.273	2.000	1.049	101.0	0.049	1034	0.0	14.0	0.25	0.0	0.0	0.0	0	0.0	0.0	0	1
2	0.300	2.000	1.033	101.0	0.049	1034	0.0	20.0	0.25	0.0	0.0	0.0	0	0.0	0.0	0	1
3	0.218	1.374	1.199	101.0	0.047	1034	0.0	7.0	0.25	0.0	0.0	0.0	0	0.0	0.0	0	1
4	0.218	1.374	1.199	101.0	0.043	1034	0.0	7.0	0.25	0.0	0.0	0.0	0	0.0	0.0	0	1
...	...	...	...	...	...	...	...	...	...	...	...	...	...	...	...	...	...
641	0.200	0.000	1.040	15.0	0.063	800	0.2	0.6	0.00	0.0	1.0	36.0	6	0.0	0.0	0	1
642	0.200	0.000	1.040	15.0	0.065	800	0.2	0.6	0.00	0.0	1.5	36.0	6	0.0	0.0	0	1
643	0.200	0.000	1.040	15.0	0.066	800	0.2	0.6	0.00	0.0	2.0	36.0	6	0.0	0.0	0	1
644	0.200	0.000	1.040	15.0	0.064	800	0.2	0.6	0.00	0.0	2.5	36.0	6	0.0	0.0	0	1
645	0.200	0.000	1.040	15.0	0.066	800	0.2	0.6	0.00	0.0	3.0	36.0	6	0.0	0.0	0	0

646 rows × 17 columns

In [3]:

```
Statistical_data=fire.agg(
    {
"Water/binder ratio (%)":["min", "max", "median", "skew","std","mean" ],
"Aggregate/binder ratio (%)":["min", "max", "median", "skew", "std","mean" ],
"Sand/binder ratio (%)":["min", "max", "median", "skew", "std","mean" ],
"Heating rate (C/min)":["min", "max", "median", "skew", "std","mean" ],
"Moisture content":["min", "max", "median", "skew", "std","mean" ],
"Maximum exposure temperature (C)":["min", "max","median","skew","std","mean"],
"Silica fume/binder ratio (%)":["min", "max", "median", "skew", "std","mean" ],
"Aggregate size (mm)":["min", "max", "median", "skew", "std","mean" ],
"GGBS/binder ratio (%)":["min", "max", "median", "skew", "std","mean" ],
"FA/binder ratio (%)":["min", "max", "median", "skew", "std","mean" ],
"PP fiber quantity (kg/m3)":["min", "max", "median", "skew", "std","mean" ],
```

This is a preprint draft. The published article can be found at: https://doi.org/10.1016/j.conbuildmat.2022.128648.

Please cite this paper as:

Al-Bashiti, M., Naser, M.Z. (2022). Verifying Domain Knowledge and Theories on Fire-induced Spalling of Concrete through eXplainable Artificial Intelligence. *Construction and Building Materials*. https://doi.org/10.1016/j.conbuildmat.2022.128648.

```
"PP fiber diameter(um)":["min", "max", "median", "skew", "std","mean" ],
"PP fiber length (mm)":["min", "max", "median", "skew", "std","mean" ],
"Steel fiber quantity (kg/m3)":["min", "max", "median", "skew", "std","mean" ],
"Steel fiber diameter(mm)":["min", "max", "median", "skew", "std","mean" ],
"Steel fiber length (mm)":["min", "max", "median", "skew", "std","mean" ],
    }
)

Statistical_data
```

Out[3]:

	Water/binder ratio (%)	Aggregate/binder ratio (%)	Sand/binder ratio (%)	Heating rate (C/min)	Moisture content	Maximum exposure temperature (C)	Silica fume/binder ratio (%)	Aggregate size (mm)	GGBS/binder ratio (%)	FA/binder ratio (%)	PP fiber quantity (kg/m3)	PP fiber diameter(um)	PP fiber length (mm)	Steel fiber quantity (kg/m3)	Steel fiber diameter(mm)	Steel fiber length (mm)
min	0.115000	0.000000	0.345000	0.250000	0.000000	100.000000	0.000000	0.120000	0.000000	0.000000	0.000000	0.000000	0.000000	0.000000	0.000000	0.000000
max	0.610000	3.952000	3.380000	240.000000	0.073000	1200.000000	0.232000	32.000000	0.458000	0.700000	14.560000	100.000000	15.000000	243.000000	1.000000	60.000000
median	0.269000	1.278000	1.222000	7.000000	0.030000	600.000000	0.000000	8.000000	0.000000	0.000000	0.000000	0.000000	0.000000	0.000000	0.000000	0.000000
skew	0.930188	0.432825	1.343488	2.934597	0.125288	0.133034	0.703968	0.519470	2.536328	3.725072	3.496500	2.018732	1.151806	1.350982	2.113286	2.378974
std	0.120693	1.123410	0.553301	36.926746	0.022791	234.322744	0.088351	7.601413	0.095737	0.112682	1.912621	17.184847	4.427905	76.755249	0.206403	10.250184
mean	0.290080	1.150981	1.404385	20.845201	0.027529	561.281734	0.070331	8.255975	0.038320	0.040319	0.966749	11.433746	3.123839	51.482972	0.128854	6.300310

In [4]:

```
x=fire.drop(['Output'],axis=1)
y=fire['Output']
x_train,x_test,y_train,y_test=train_test_split(x,y,test_size=0.30,random_state=111)
```

In [5]:

```
for i, col in enumerate(fire.columns):
    pyplot.figure(i)
    sns.histplot(fire[col])
```

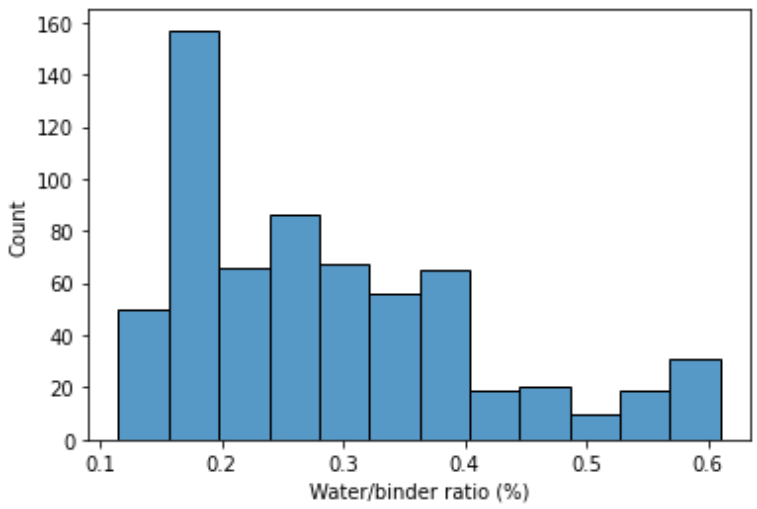

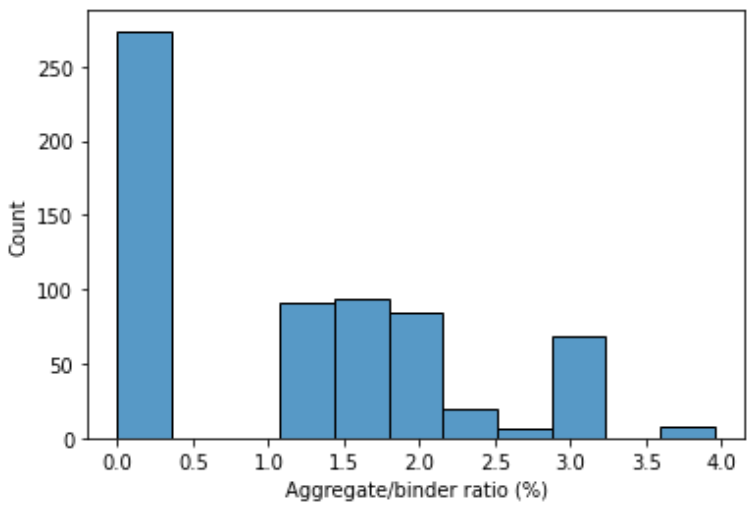

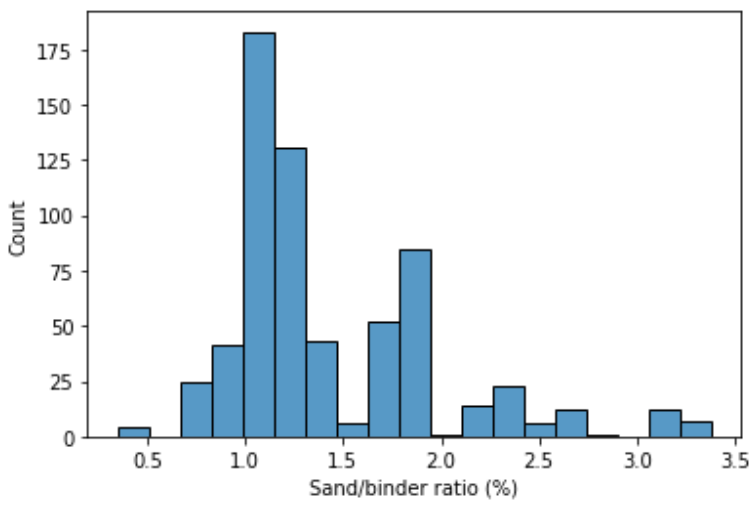

This is a preprint draft. The published article can be found at: https://doi.org/10.1016/j.conbuildmat.2022.128648.

Please cite this paper as:

Al-Bashiti, M., Naser, M.Z. (2022). Verifying Domain Knowledge and Theories on Fire-induced Spalling of Concrete through eXplainable Artificial Intelligence. *Construction and Building Materials*. https://doi.org/10.1016/j.conbuildmat.2022.128648.

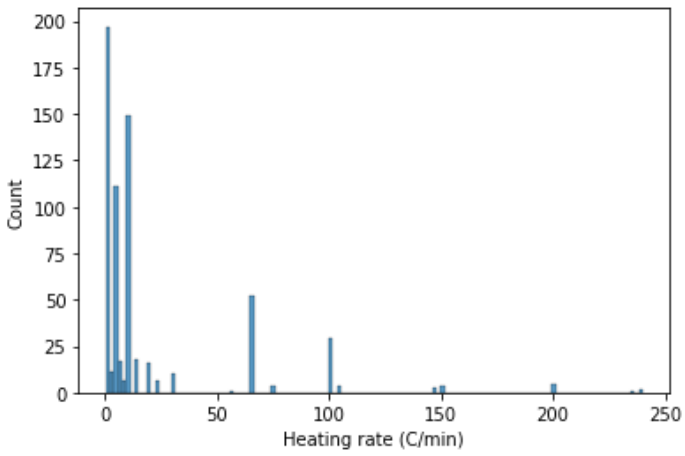

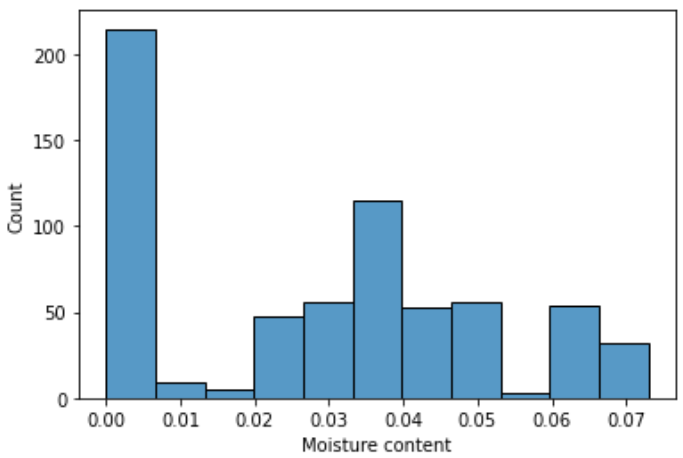

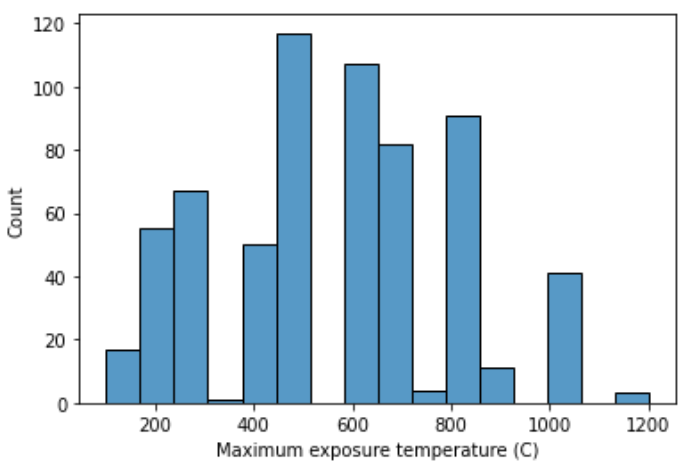

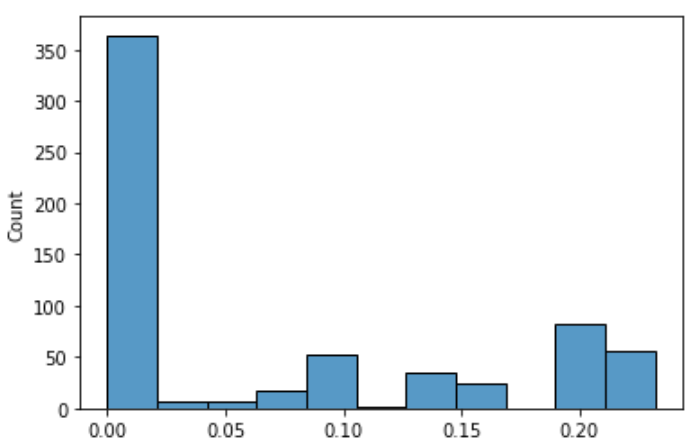

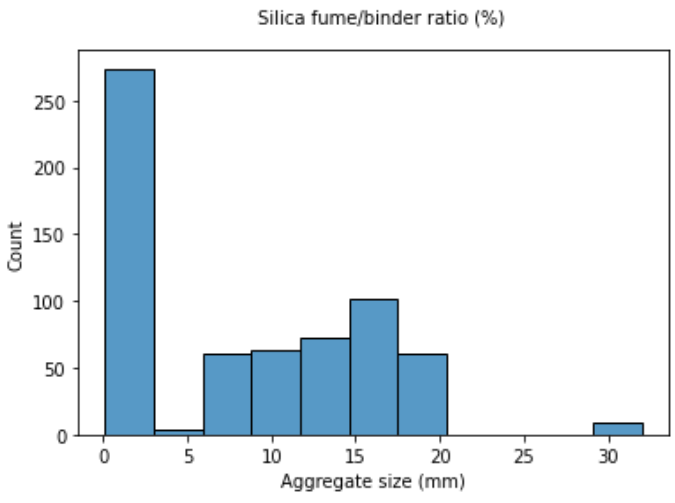

This is a preprint draft. The published article can be found at: https://doi.org/10.1016/j.conbuildmat.2022.128648.

Please cite this paper as:

Al-Bashiti, M., Naser, M.Z. (2022). Verifying Domain Knowledge and Theories on Fire-induced Spalling of Concrete through eXplainable Artificial Intelligence. *Construction and Building Materials*. https://doi.org/10.1016/j.conbuildmat.2022.128648.

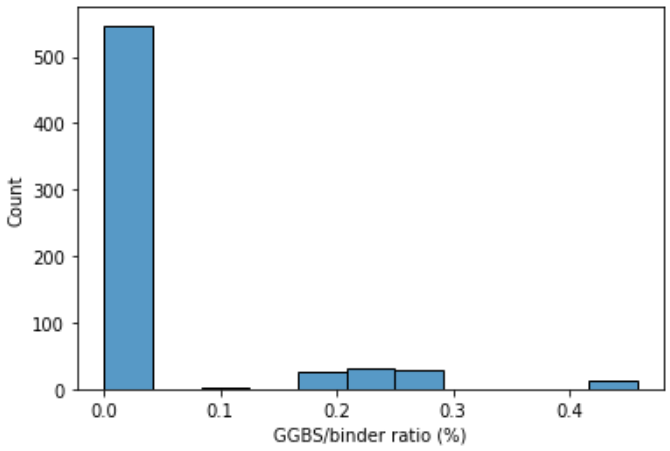

643

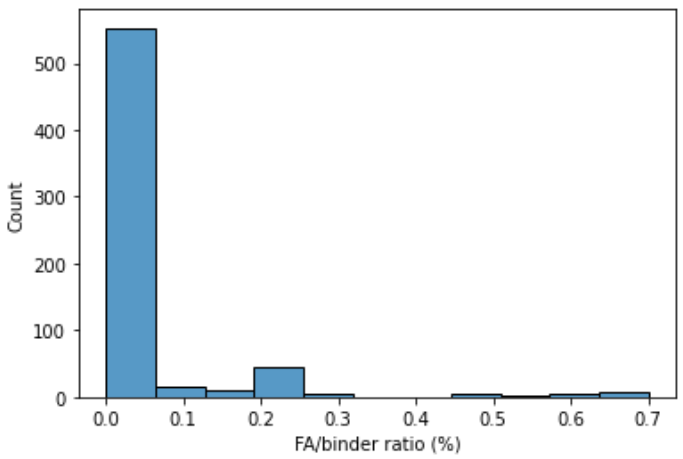

644

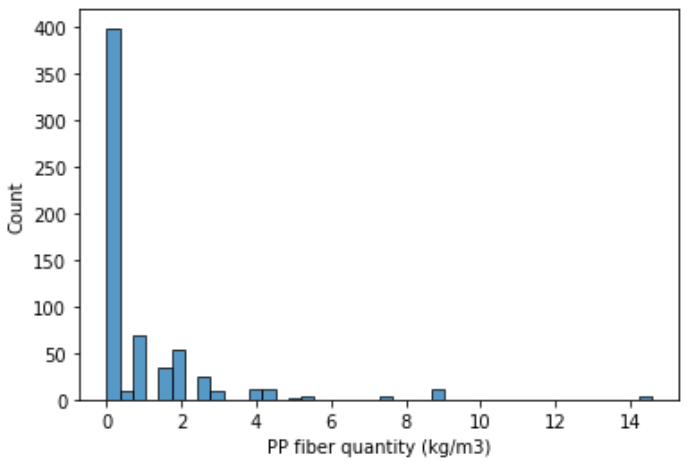

645

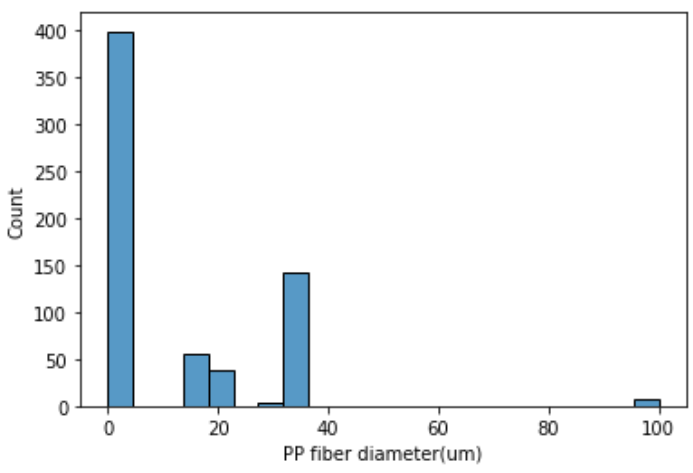

646

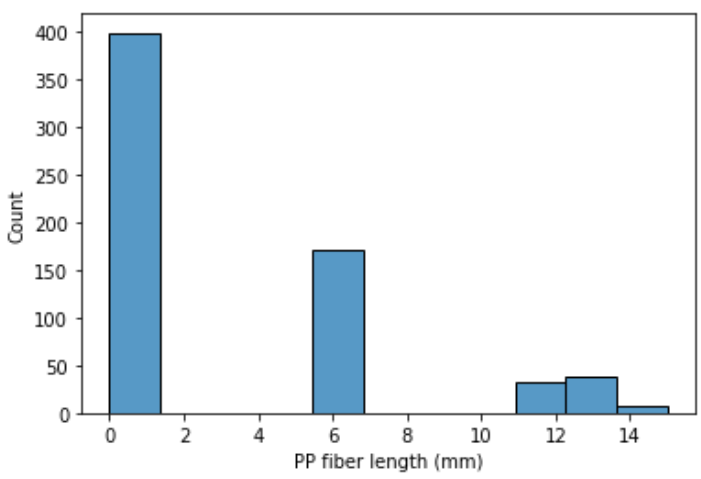

647

This is a preprint draft. The published article can be found at: https://doi.org/10.1016/j.conbuildmat.2022.128648.

Please cite this paper as:

Al-Bashiti, M., Naser, M.Z. (2022). Verifying Domain Knowledge and Theories on Fire-induced Spalling of Concrete through eXplainable Artificial Intelligence. *Construction and Building Materials*. https://doi.org/10.1016/j.conbuildmat.2022.128648.

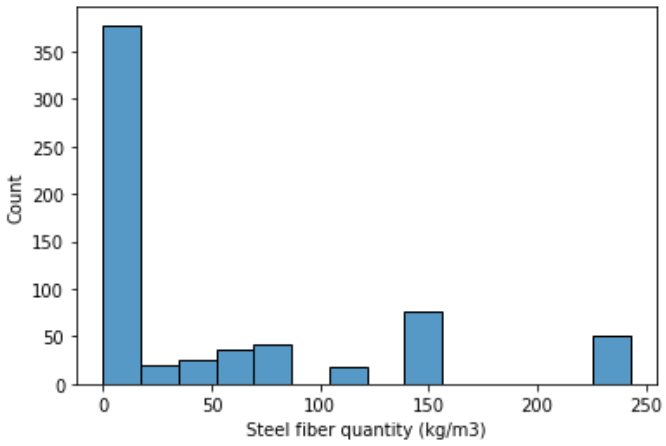

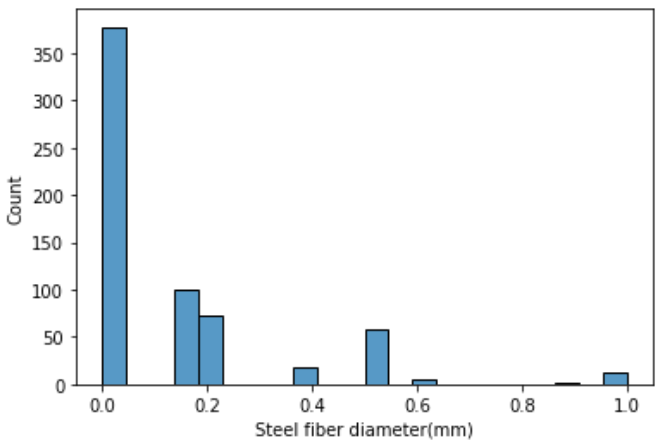

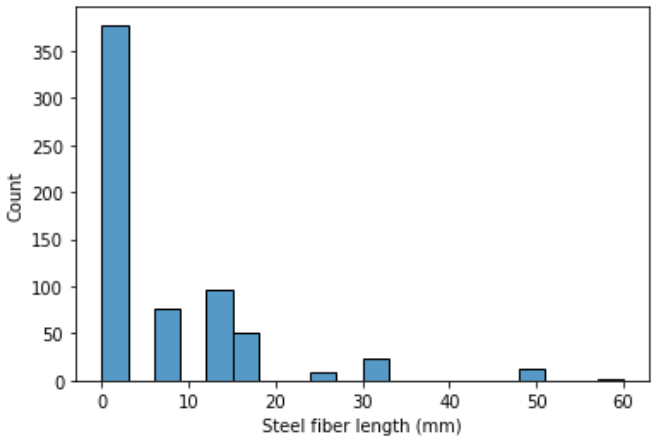

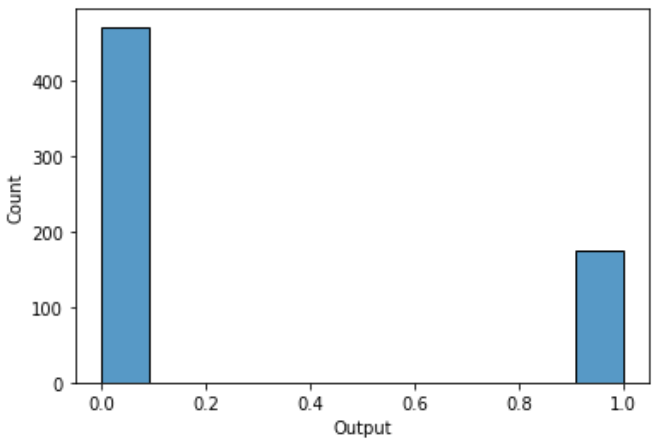

In [6]:

```
xgbc=xgb.XGBClassifier(objective ='binary:logistic' ,missing=1,seed=42
                       ,learning_rate = 0.05 , max_depth = 3)
xgbc.fit(x_train,y_train,verbose=True,early_stopping_rounds=50,
         eval_metric='aucpr',eval_set=[(x_test,y_test)])
predictions = xgbc.predict(x_test)
kfold = StratifiedKFold(n_splits=10, random_state=7,shuffle=True)
results = cross_val_score(xgbc, x, y, cv=kfold)
print("Accuracy: %.2f%% (%.2f%%)" % (results.mean()*100, results.std()*100))
```

```
[0]     validation_0-aucpr:0.70297
[1]     validation_0-aucpr:0.70297
[2]     validation_0-aucpr:0.74610
[3]     validation_0-aucpr:0.83571
[4]     validation_0-aucpr:0.83334
[5]     validation_0-aucpr:0.84276
[6]     validation_0-aucpr:0.85755
[7]     validation_0-aucpr:0.84832
[8]     validation_0-aucpr:0.85179
[9]     validation_0-aucpr:0.85191
[10]    validation_0-aucpr:0.85738
[11]    validation_0-aucpr:0.85867
[12]    validation_0-aucpr:0.86494
[13]    validation_0-aucpr:0.86189
[14]    validation_0-aucpr:0.86285
[15]    validation_0-aucpr:0.86467
[16]    validation_0-aucpr:0.86886
```

```
[17]    validation_0-aucpr:0.87422
[18]    validation_0-aucpr:0.88066
[19]    validation_0-aucpr:0.87465
[20]    validation_0-aucpr:0.88346
[21]    validation_0-aucpr:0.88151
[22]    validation_0-aucpr:0.88042
[23]    validation_0-aucpr:0.88075
[24]    validation_0-aucpr:0.88423
[25]    validation_0-aucpr:0.88324
[26]    validation_0-aucpr:0.88595
[27]    validation_0-aucpr:0.88528
[28]    validation_0-aucpr:0.88997
[29]    validation_0-aucpr:0.88982
[30]    validation_0-aucpr:0.89384
[31]    validation_0-aucpr:0.89392
[32]    validation_0-aucpr:0.89683
[33]    validation_0-aucpr:0.89732
[34]    validation_0-aucpr:0.90004
[35]    validation_0-aucpr:0.90253
[36]    validation_0-aucpr:0.90414
[37]    validation_0-aucpr:0.90404
[38]    validation_0-aucpr:0.90708
[39]    validation_0-aucpr:0.90555
[40]    validation_0-aucpr:0.90795
[41]    validation_0-aucpr:0.90796
[42]    validation_0-aucpr:0.90886
[43]    validation_0-aucpr:0.91232
[44]    validation_0-aucpr:0.90999
[45]    validation_0-aucpr:0.91347
[46]    validation_0-aucpr:0.91142
[47]    validation_0-aucpr:0.91566
[48]    validation_0-aucpr:0.91499
[49]    validation_0-aucpr:0.91832
[50]    validation_0-aucpr:0.92337
[51]    validation_0-aucpr:0.92183
[52]    validation_0-aucpr:0.92448
[53]    validation_0-aucpr:0.92428
[54]    validation_0-aucpr:0.92148
[55]    validation_0-aucpr:0.92306
[56]    validation_0-aucpr:0.92386
[57]    validation_0-aucpr:0.92858
[58]    validation_0-aucpr:0.92860
[59]    validation_0-aucpr:0.93117
[60]    validation_0-aucpr:0.93456
[61]    validation_0-aucpr:0.93367
[62]    validation_0-aucpr:0.93503
[63]    validation_0-aucpr:0.93172
[64]    validation_0-aucpr:0.93481
[65]    validation_0-aucpr:0.93518
[66]    validation_0-aucpr:0.93658
[67]    validation_0-aucpr:0.93680
[68]    validation_0-aucpr:0.93404
[69]    validation_0-aucpr:0.93882
[70]    validation_0-aucpr:0.94006
[71]    validation_0-aucpr:0.93848
[72]    validation_0-aucpr:0.93876
[73]    validation_0-aucpr:0.94026
[74]    validation_0-aucpr:0.94022
[75]    validation_0-aucpr:0.93997
[76]    validation_0-aucpr:0.93832
[77]    validation_0-aucpr:0.94102
[78]    validation_0-aucpr:0.94168
[79]    validation_0-aucpr:0.94359
[80]    validation_0-aucpr:0.94418
[81]    validation_0-aucpr:0.94495
[82]    validation_0-aucpr:0.94636
[83]    validation_0-aucpr:0.94617
[84]    validation_0-aucpr:0.94617
[85]    validation_0-aucpr:0.94617
[86]    validation_0-aucpr:0.94636
[87]    validation_0-aucpr:0.94782
[88]    validation_0-aucpr:0.94856
[89]    validation_0-aucpr:0.94732
[90]    validation_0-aucpr:0.94732
[91]    validation_0-aucpr:0.94732
[92]    validation_0-aucpr:0.94887
[93]    validation_0-aucpr:0.94826
[94]    validation_0-aucpr:0.95129
[95]    validation_0-aucpr:0.95190
[96]    validation_0-aucpr:0.95129
[97]    validation_0-aucpr:0.94883
[98]    validation_0-aucpr:0.94975
```

This is a preprint draft. The published article can be found at: https://doi.org/10.1016/j.conbuildmat.2022.128648.

Please cite this paper as:

Al-Bashiti, M., Naser, M.Z. (2022). Verifying Domain Knowledge and Theories on Fire-induced Spalling of Concrete through eXplainable Artificial Intelligence. *Construction and Building Materials*. https://doi.org/10.1016/j.conbuildmat.2022.128648.

```
[99]    validation_0-aucpr:0.95032
Accuracy: 88.09% (2.64%)
```

In [7]:

```
class_names = ['no spalling ', 'spallling']
disp = plot_confusion_matrix(xgbc, x_test, y_test, display_labels=class_names, cmap=pyplot.cm.Blues,
xticks_rotation='vertical')
pyplot.title('Testing set')
print (classification_report(y_test,predictions))
```

```
              precision    recall  f1-score   support

           0       0.90      0.97      0.94       135
           1       0.92      0.76      0.83        59

    accuracy                           0.91       194
   macro avg       0.91      0.87      0.88       194
weighted avg       0.91      0.91      0.90       194
```

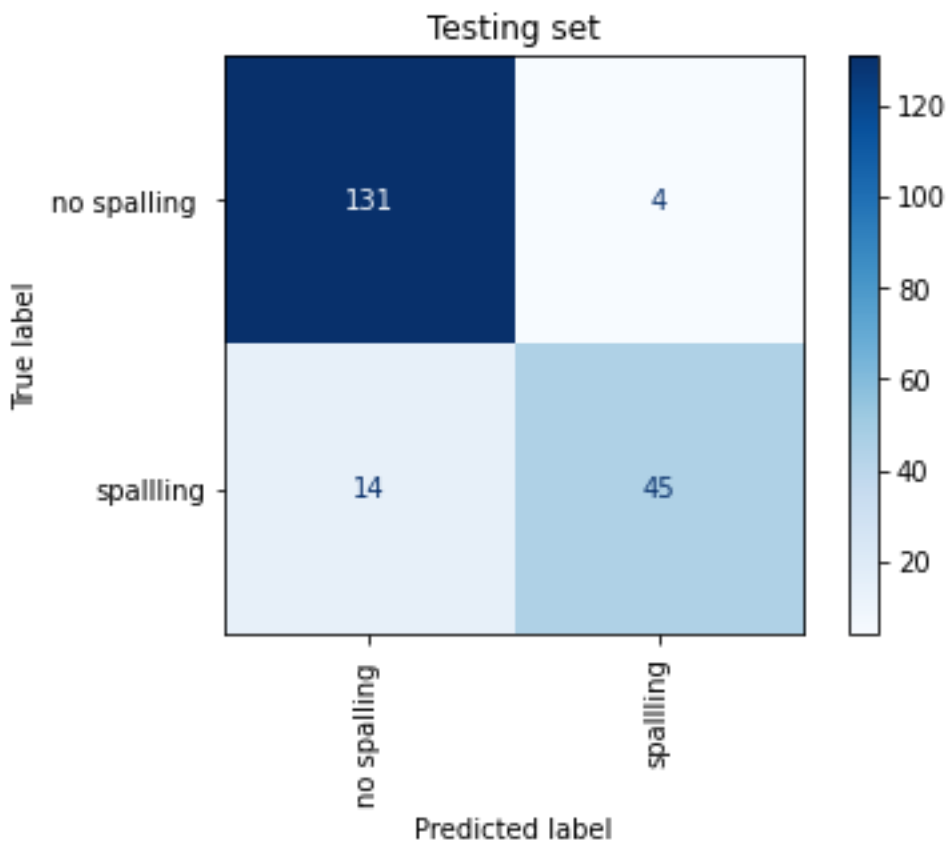

In [8]:

```
class_names = ['no spalling ', 'spallling']
disp = plot_confusion_matrix(xgbc, x_train, y_train, display_labels=class_names,colorbar=True, cmap=pyplot.cm.Blues,
xticks_rotation='vertical')
pyplot.title('Training set')
```

Out[8]:

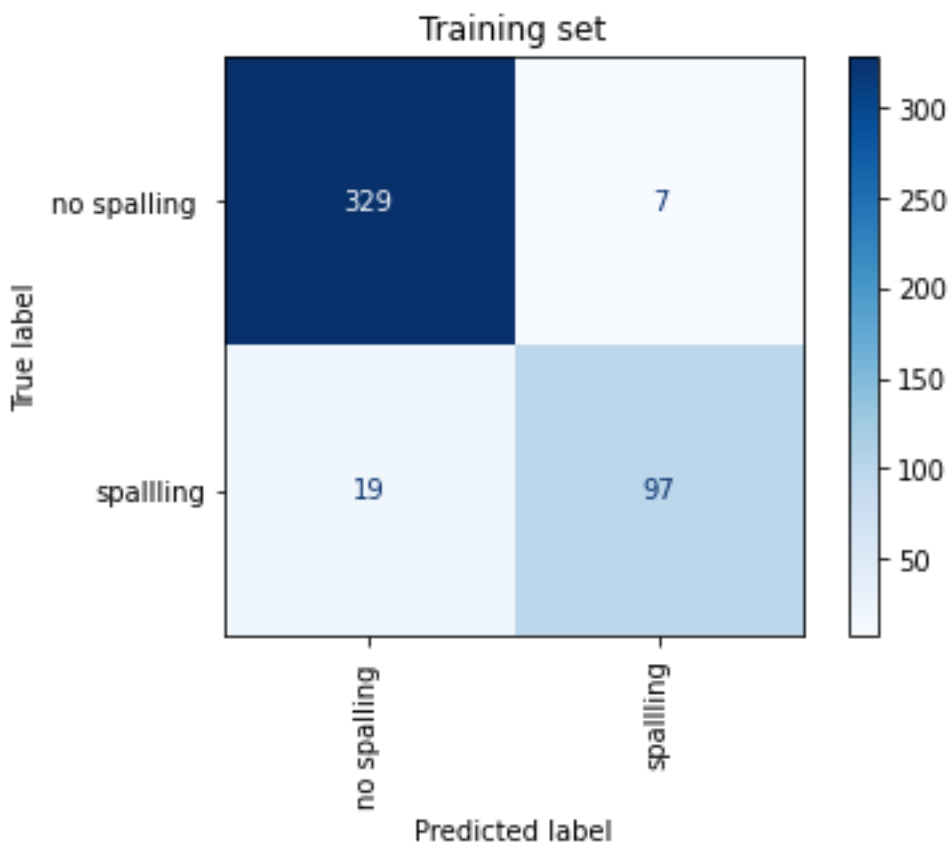

In [9]:

```
r_auc=roc_auc_score(y_test,predictions)
r_auc
```

Out[9]:

```
0.866541117388575
```

In [10]:

```
yhat = xgbc.predict_proba(x_test)

# retrieve just the probabilities for the positive class
pos_probs = yhat[:, 1]
# plot no skill roc curve
pyplot.plot([0, 1], [0, 1], linestyle='--')
# calculate roc curve for model
fpr, tpr, _ = roc_curve(y_test, pos_probs)
# plot model roc curve
pyplot.plot(fpr, tpr, marker='.', label='AUC=0.866')
# axis labels
pyplot.xlabel('False Positive Rate')
pyplot.ylabel('True Positive Rate')
# show the legend
pyplot.legend()
pyplot.title('Testing set')
# show the plot
pyplot.show()
```

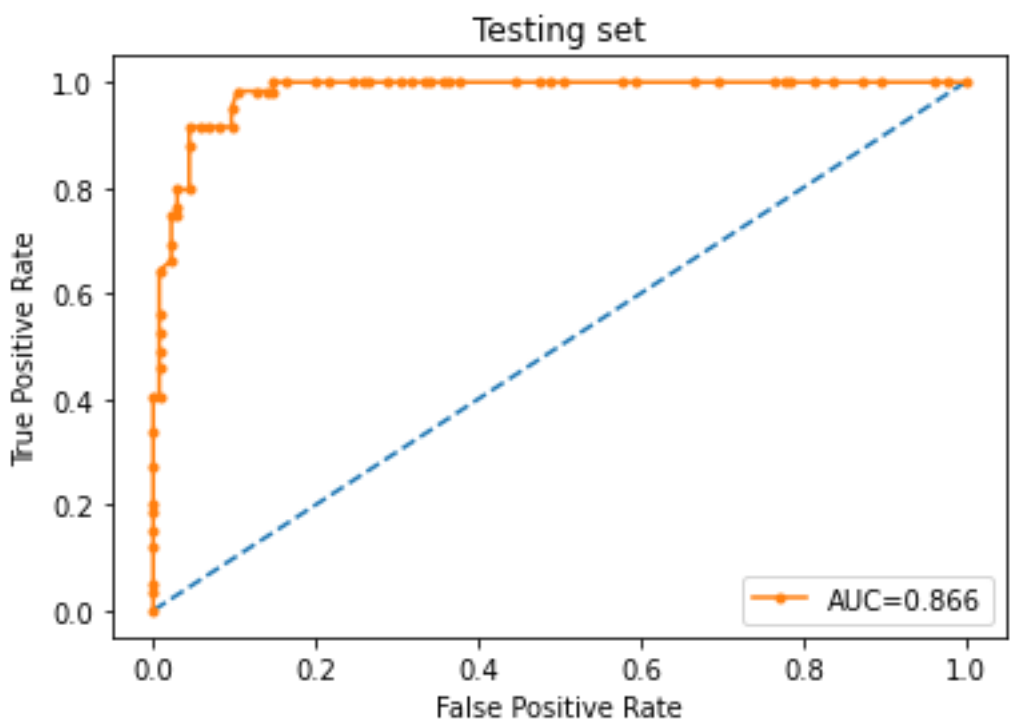

In [11]:

```
yhat = xgbc.predict_proba(x_train)

# retrieve just the probabilities for the positive class
pos_probs = yhat[:, 1]
# plot no skill roc curve
pyplot.plot([0, 1], [0, 1], linestyle='--')
# calculate roc curve for model
fpr, tpr, _ = roc_curve(y_train, pos_probs)
# plot model roc curve
pyplot.plot(fpr, tpr, marker='.', label='AUC=0.907')
# axis labels
pyplot.xlabel('False Positive Rate')
pyplot.ylabel('True Positive Rate')
# show the legend
pyplot.legend()
pyplot.title('Training set')
# show the plot
pyplot.show()
```

This is a preprint draft. The published article can be found at: https://doi.org/10.1016/j.conbuildmat.2022.128648.

Please cite this paper as:

Al-Bashiti, M., Naser, M.Z. (2022). Verifying Domain Knowledge and Theories on Fire-induced Spalling of Concrete through eXplainable Artificial Intelligence. *Construction and Building Materials*. https://doi.org/10.1016/j.conbuildmat.2022.128648.

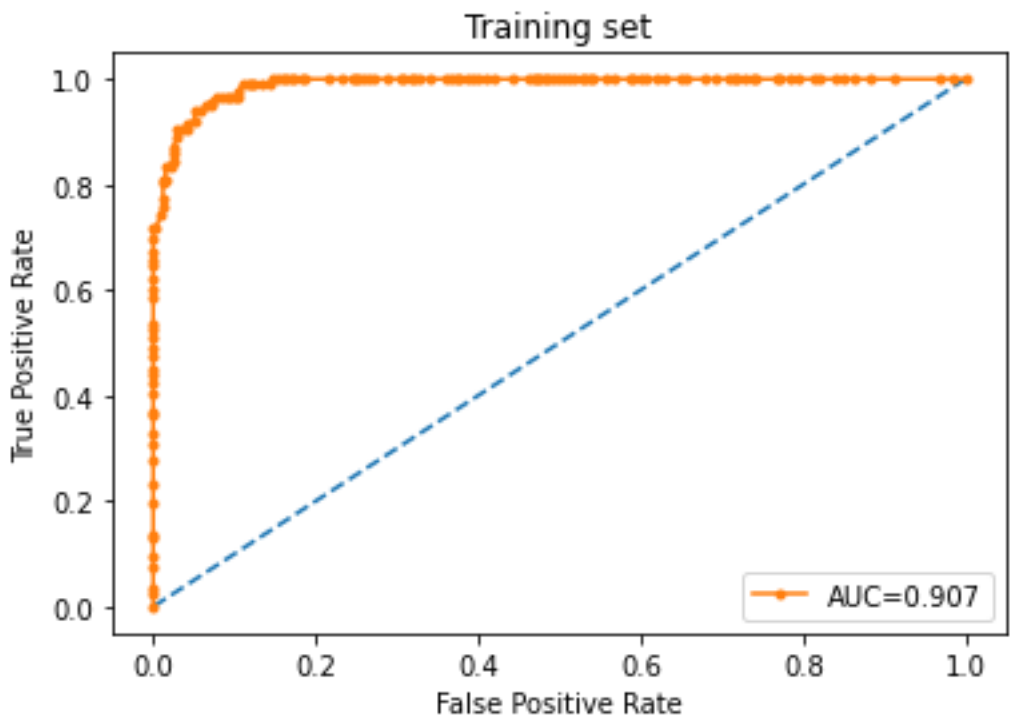

In [12]:

```
importances = xgbc.feature_importances_
indices = np.argsort(importances)
features = x.columns
pyplot.title('Feature Importances')
pyplot.barh(range(len(indices)), importances[indices], color='g', align='center')
pyplot.yticks(range(len(indices)), [features[i] for i in indices])
pyplot.xlabel('Relative Importance')
pyplot.show()
```

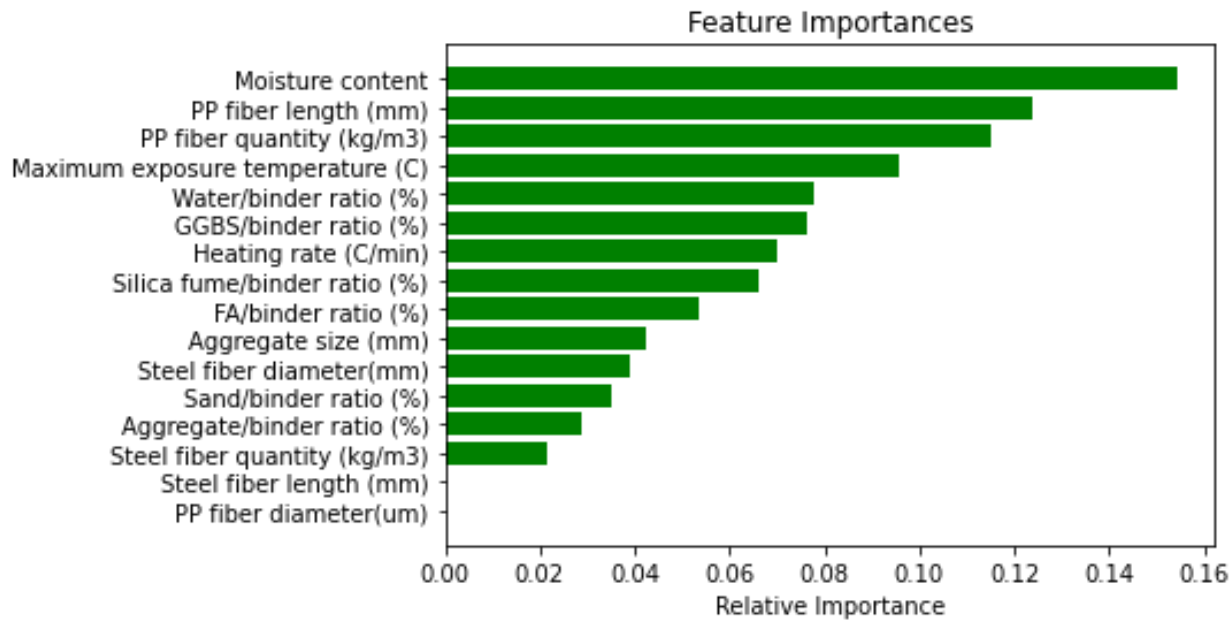

In [13]:

```
l=fire.corr()
```

In [14]:

```
sns.heatmap(l, annot=True)
sns.set(rc = {'figure.figsize':(22,12)})
pyplot.title("Pearson Correlation")

pyplot.show()
```

This is a preprint draft. The published article can be found at: https://doi.org/10.1016/j.conbuildmat.2022.128648.

Please cite this paper as:

Al-Bashiti, M., Naser, M.Z. (2022). Verifying Domain Knowledge and Theories on Fire-induced Spalling of Concrete through eXplainable Artificial Intelligence. *Construction and Building Materials*. https://doi.org/10.1016/j.conbuildmat.2022.128648.

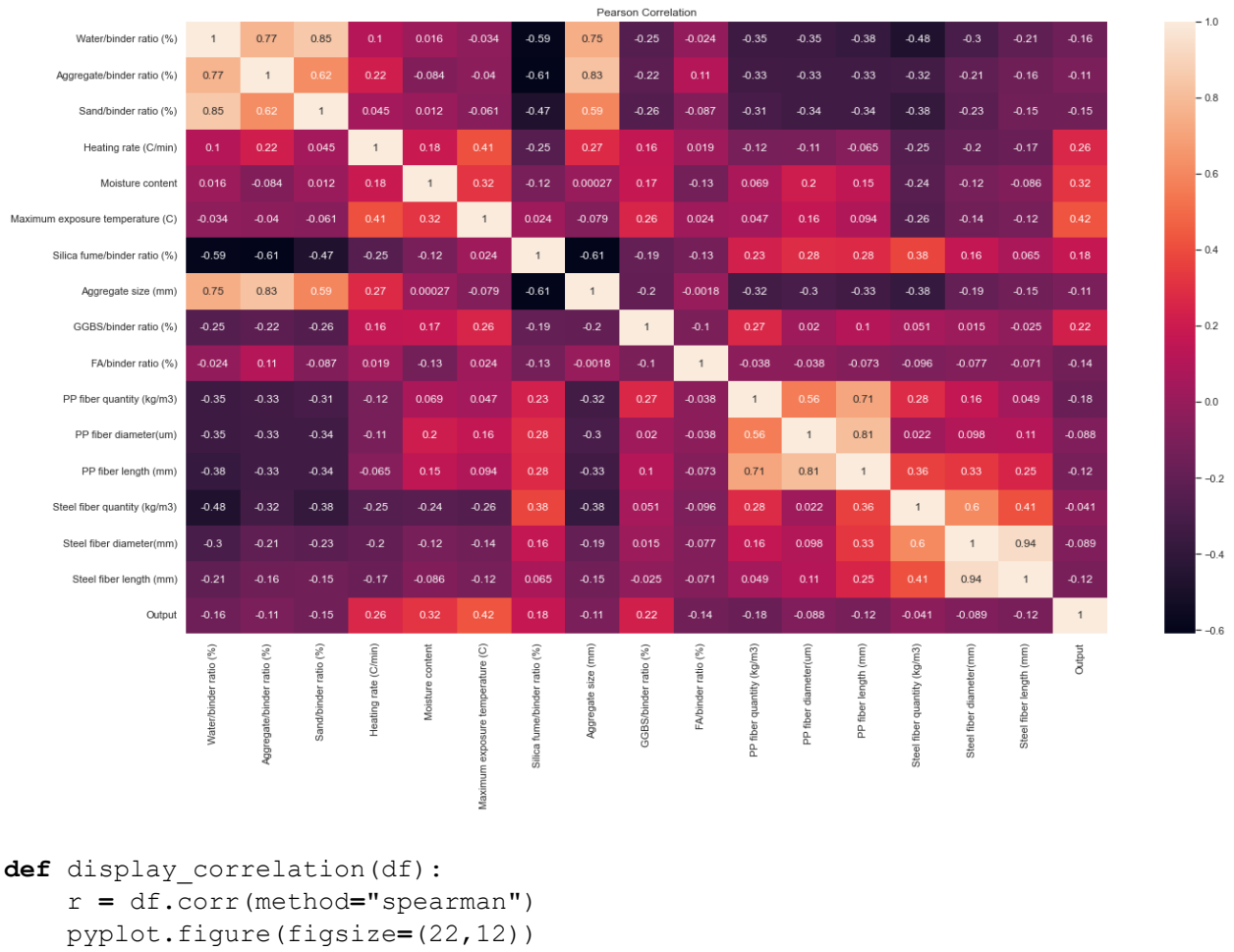

In [15]:

```
def display_correlation(df):
    r = df.corr(method="spearman")
    pyplot.figure(figsize=(22,12))
    heatmap = sns.heatmap(df.corr(), vmin=-1,
                          vmax=1, annot=True)
    pyplot.title("Spearman Correlation")
    return(r)

r_simple=display_correlation(l)
```

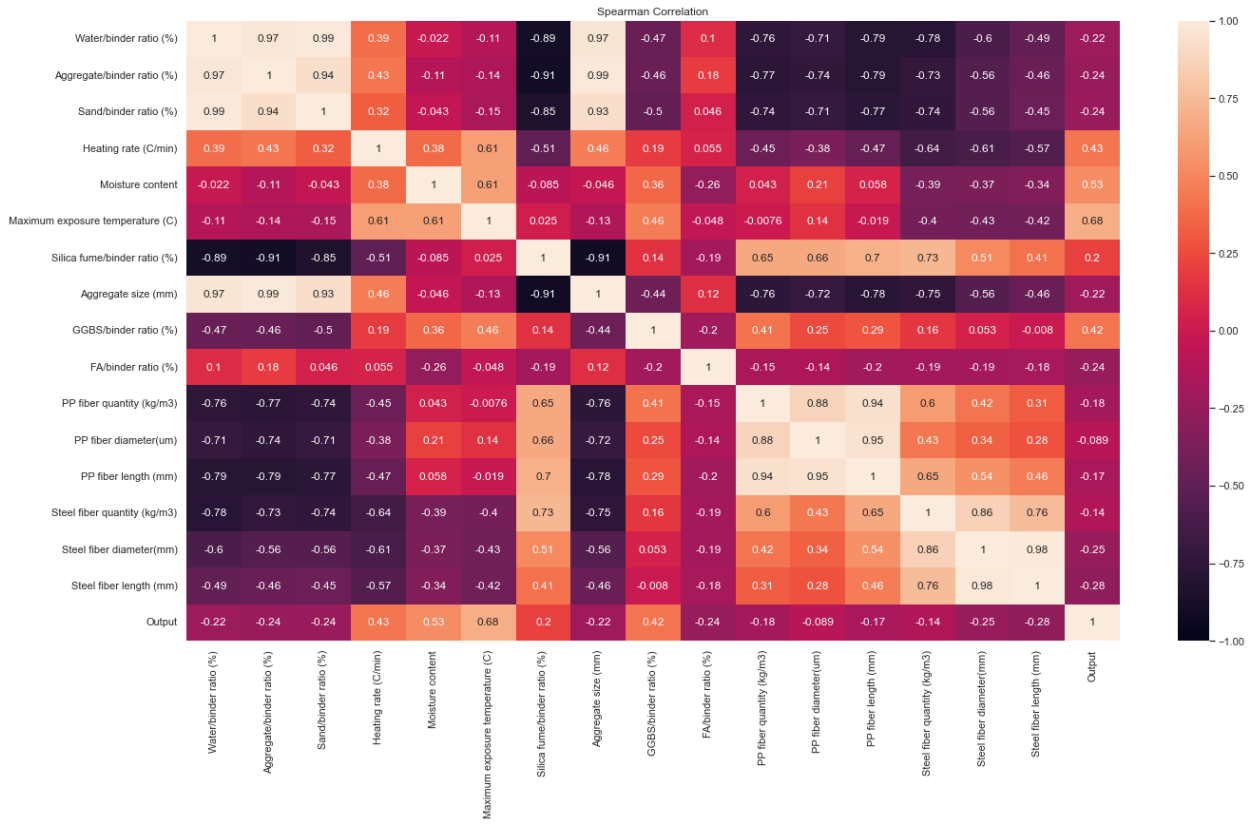

In [16]:

```
import shap
shap.initjs()

explainer = shap.TreeExplainer(xgbc)
shap_values = explainer.shap_values(x_test)
shap.summary_plot(shap_values, x_test, plot_type="bar")
```

This is a preprint draft. The published article can be found at: https://doi.org/10.1016/j.conbuildmat.2022.128648.

Please cite this paper as:

Al-Bashiti, M., Naser, M.Z. (2022). Verifying Domain Knowledge and Theories on Fire-induced Spalling of Concrete through eXplainable Artificial Intelligence. *Construction and Building Materials*. https://doi.org/10.1016/j.conbuildmat.2022.128648.

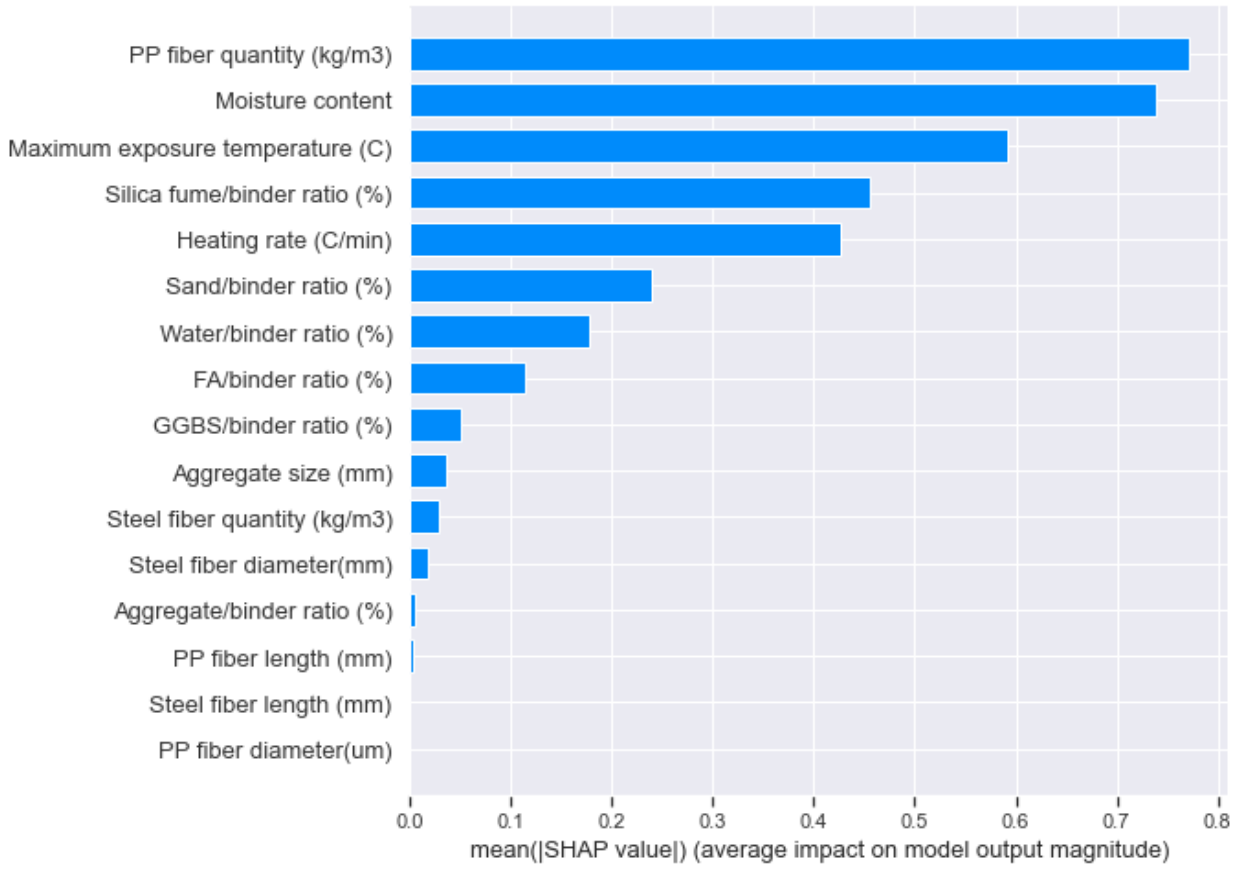

In [17]:

```
shap.summary_plot(shap_values, x_test,show=False)
pyplot.gcf().axes[-1].set_box_aspect(50)
pyplot.gcf().axes[-1].set_aspect(100)
pyplot.gcf().axes[-1].set_box_aspect(100)
```

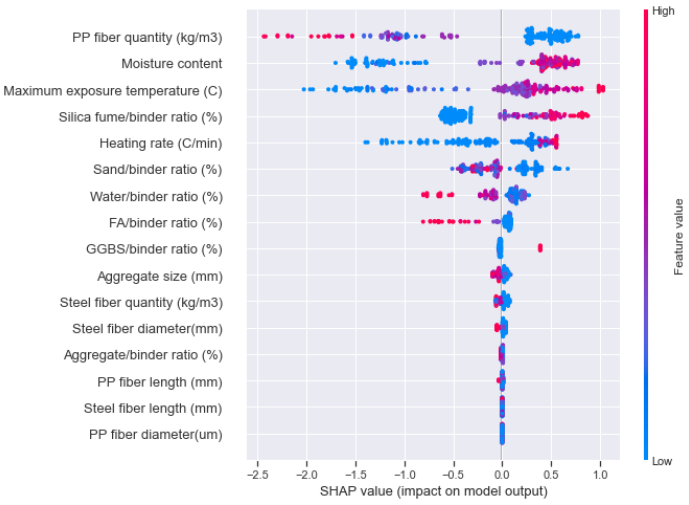

In [18]:

```
xgb_binary_shap_values = explainer(x_test)
```

In [19]:

```
def xgb_shap_transform_scale(original_shap_values, Y_pred, which):
    from scipy.special import expit
    #Compute the transformed base value, which consists in applying the logit function to the base value
    from scipy.special import expit #Importing the logit function for the base value transformation
    untransformed_base_value = original_shap_values.base_values[-1]

    #Computing the original_explanation_distance to construct the distance_coefficient later on
    original_explanation_distance = np.sum(original_shap_values.values, axis=1)[which]

    base_value = expit(untransformed_base_value ) # = 1 / (1+ np.exp(-untransformed_base_value))

    #Computing the distance between the model_prediction and the transformed base_value
    distance_to_explain = Y_pred[which] - base_value

    #The distance_coefficient is the ratio between both distances which will be used later on
    distance_coefficient = original_explanation_distance / distance_to_explain

    #Transforming the original shapley values to the new scale
    shap_values_transformed = original_shap_values / distance_coefficient

    #Finally resetting the base_value as it does not need to be transformed
    shap_values_transformed.base_values = base_value
    shap_values_transformed.data = original_shap_values.data

    #Now returning the transformed array
    return shap_values_transformed
```

In [20]:

```
obs =9

print("The prediction is ", predictions[obs])
shap_values_transformed = xgb_shap_transform_scale(xgb_binary_shap_values, predictions, obs)
shap.plots.waterfall(shap_values_transformed[obs])
shap.force_plot(shap_values_transformed[obs])
```

```
The prediction is  0
```

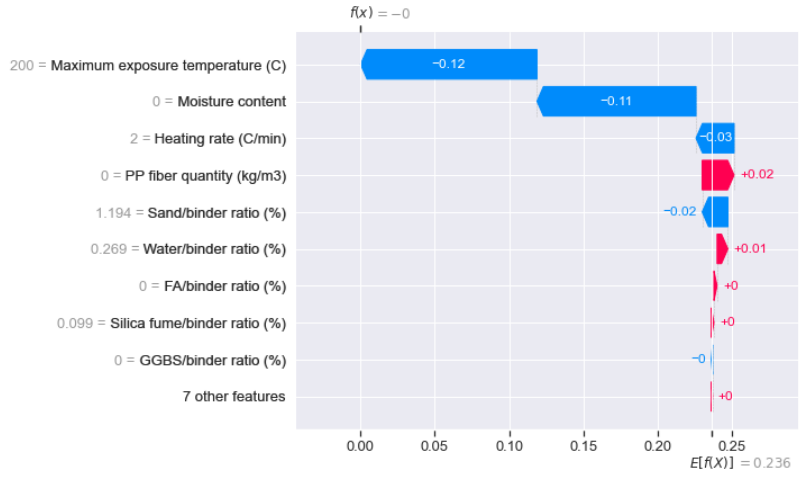

Out[20]:

In [21]:

```
obs =1

print("The prediction is ", predictions[obs])
shap_values_transformed = xgb_shap_transform_scale(xgb_binary_shap_values, predictions, obs)
shap.plots.waterfall(shap_values_transformed[obs])
shap.force_plot(shap_values_transformed[obs])
```

```
The prediction is  0
```

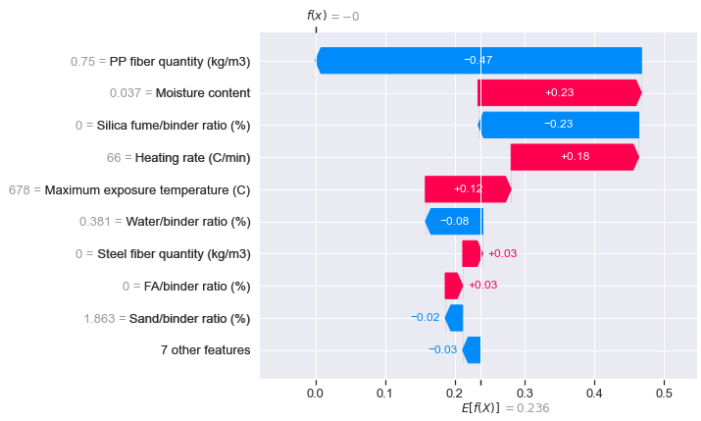

Out[21]:

In [22]:

```
obs =0

print("The prediction is ", predictions[obs])
shap_values_transformed = xgb_shap_transform_scale(xgb_binary_shap_values, predictions, obs)
shap.plots.waterfall(shap_values_transformed[obs])
shap.force_plot(shap_values_transformed[obs])
```

```
The prediction is  1
```

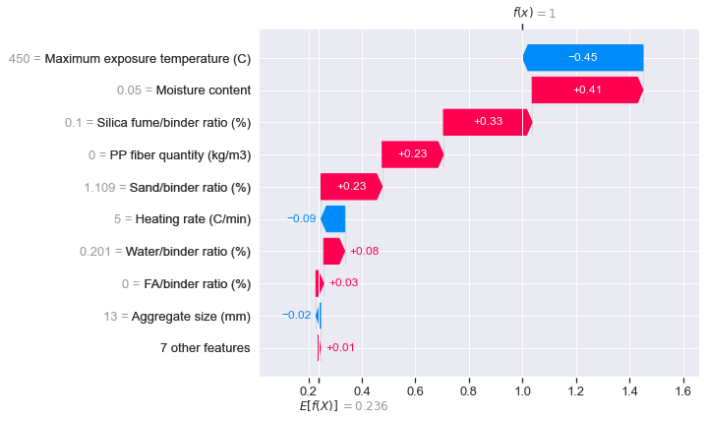

Out[22]:

In [23]:

```
obs =20

print("The prediction is ", predictions[obs])
shap_values_transformed = xgb_shap_transform_scale(xgb_binary_shap_values, predictions, obs)
shap.plots.waterfall(shap_values_transformed[obs])
shap.force_plot(shap_values_transformed[obs])
```

```
The prediction is  1
```

This is a preprint draft. The published article can be found at: https://doi.org/10.1016/j.conbuildmat.2022.128648.

Please cite this paper as:

Al-Bashiti, M., Naser, M.Z. (2022). Verifying Domain Knowledge and Theories on Fire-induced Spalling of Concrete through eXplainable Artificial Intelligence. *Construction and Building Materials*. https://doi.org/10.1016/j.conbuildmat.2022.128648.

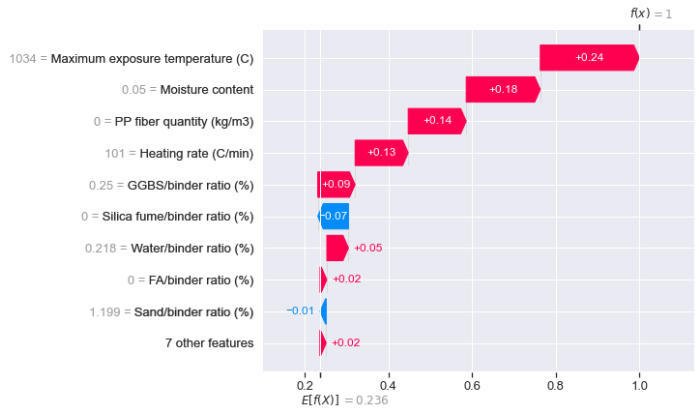

Out[23]:

In [24]:

```
obs =21

print("The prediction is ", predictions[obs])
shap_values_transformed = xgb_shap_transform_scale(xgb_binary_shap_values, predictions, obs)
shap.plots.waterfall(shap_values_transformed[obs])
shap.force_plot(shap_values_transformed[obs])
```

```
The prediction is  0
```

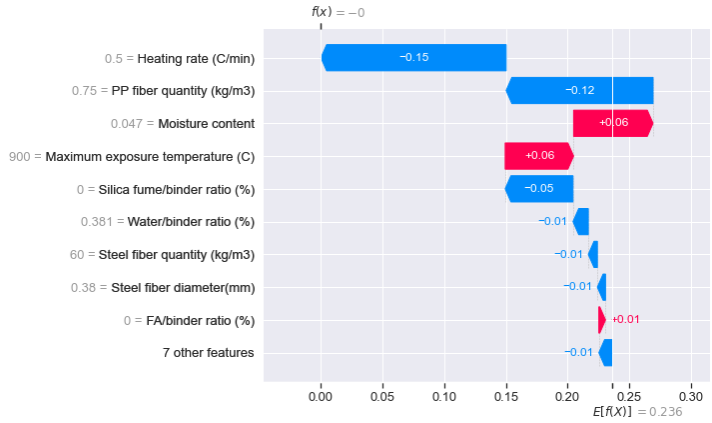

Out[24]:

In [25]:

```
import lime
import lime.lime_tabular
from lime import lime_tabular
```

In [26]:

```
explainerL = lime_tabular.LimeTabularExplainer(
    training_data=np.array(x),
    feature_names=x.columns,
    class_names=['Not spalling', 'Spalling'],
    mode='classification')
```

In [27]:

```
exp = explainerL.explain_instance(
    data_row=x.iloc[384],
    predict_fn=xgbc.predict_proba
)
#exp.save_to_file('temp.html')
exp.show_in_notebook(show_table=True)
```

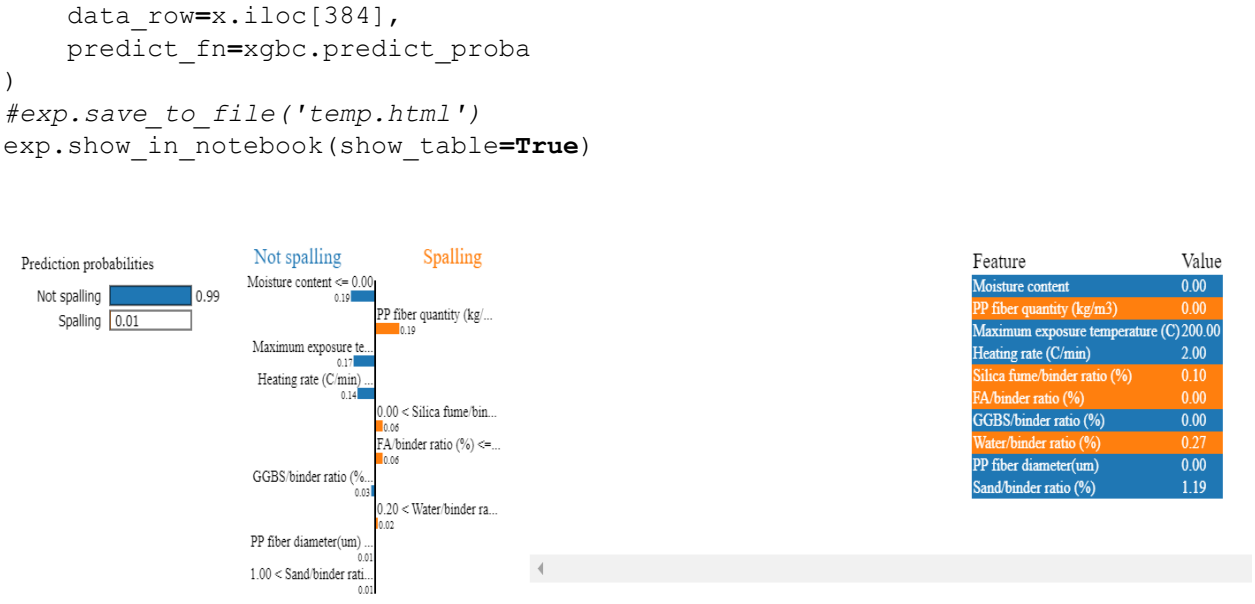

In [28]:

```
exp = explainerL.explain_instance(
    data_row=x.iloc[337],
    predict_fn=xgbc.predict_proba
)
#exp.save_to_file('temp.html')
exp.show_in_notebook(show_table=True)
```

This is a preprint draft. The published article can be found at: https://doi.org/10.1016/j.conbuildmat.2022.128648.

Please cite this paper as:

Al-Bashiti, M., Naser, M.Z. (2022). Verifying Domain Knowledge and Theories on Fire-induced Spalling of Concrete through eXplainable Artificial Intelligence. *Construction and Building Materials*. https://doi.org/10.1016/j.conbuildmat.2022.128648.

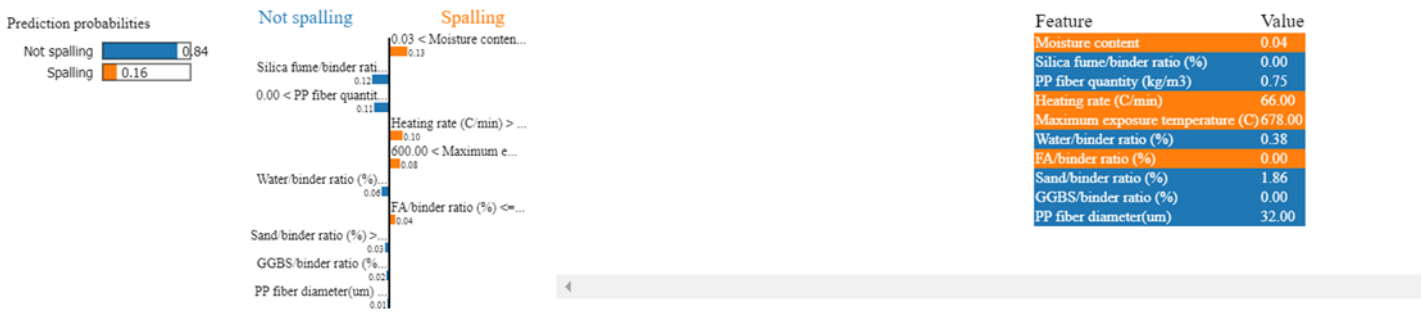

In [29]:

```
exp = explainerL.explain_instance(
    data_row=x.iloc[39],
    predict_fn=xgbc.predict_proba
)
#exp.save_to_file('temp.html')
exp.show_in_notebook(show_table=True)
```

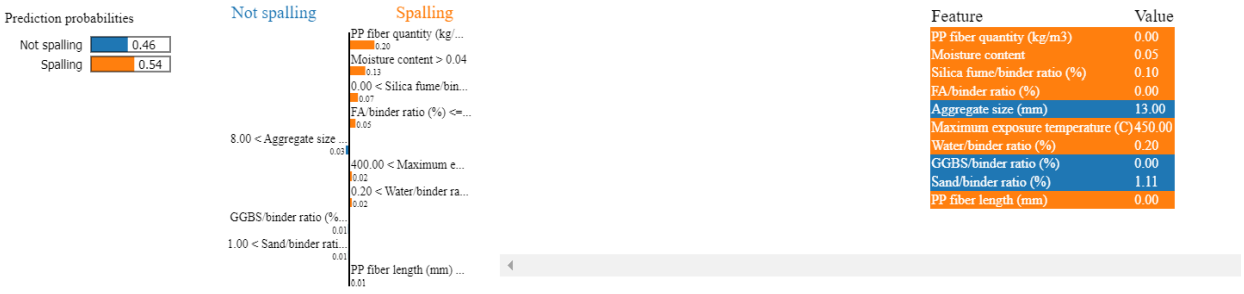

In [30]:

```
exp = explainerL.explain_instance(
    data_row=x.iloc[11],
    predict_fn=xgbc.predict_proba
)
#exp.save_to_file('temp.html')
exp.show_in_notebook(show_table=True)
```

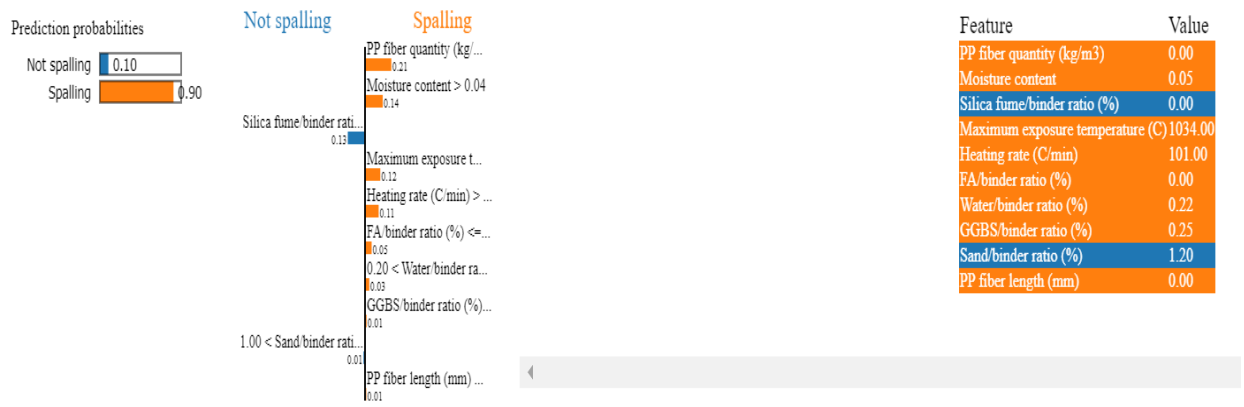

In [31]:

```
exp = explainerL.explain_instance(
    data_row=x.iloc[353],
    predict_fn=xgbc.predict_proba
)
#exp.save_to_file('temp.html')
exp.show_in_notebook(show_table=True)
```

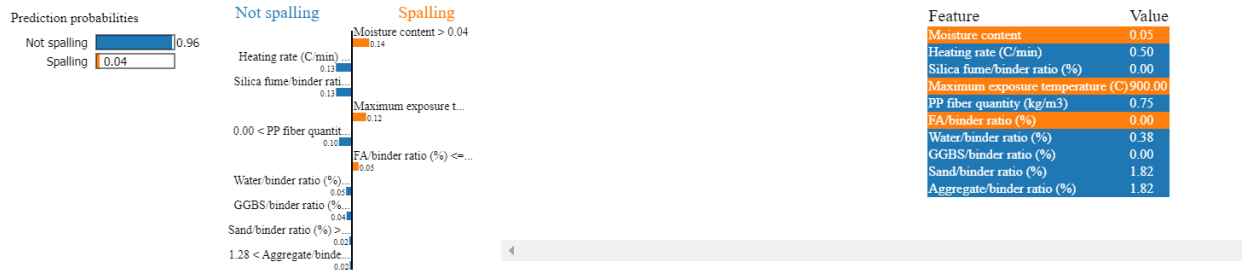

In [32]:

```
import matplotlib.pyplot as plt
from sklearn.inspection import partial_dependence
from sklearn.inspection import PartialDependenceDisplay

features = ['Moisture content',
```

This is a preprint draft. The published article can be found at: https://doi.org/10.1016/j.conbuildmat.2022.128648.

Please cite this paper as:

Al-Bashiti, M., Naser, M.Z. (2022). Verifying Domain Knowledge and Theories on Fire-induced Spalling of Concrete through eXplainable Artificial Intelligence. *Construction and Building Materials*. https://doi.org/10.1016/j.conbuildmat.2022.128648.

```
    'Water/binder ratio (%)',
    'Sand/binder ratio (%)',
    'Heating rate (C/min)',
            'Maximum exposure temperature (C)',
    'Silica fume/binder ratio (%)',
            'FA/binder ratio (%)',
    'PP fiber quantity (kg/m3)',


            ]
display = PartialDependenceDisplay.from_estimator( xgbc,x_test, features, kind="both", grid_resolution=20,
random_state=1)


for i in range(display.lines_.shape[0]):
               display.lines_[0,i,-1].set_color('Green')
               display.axes_[3, i].legend()
```

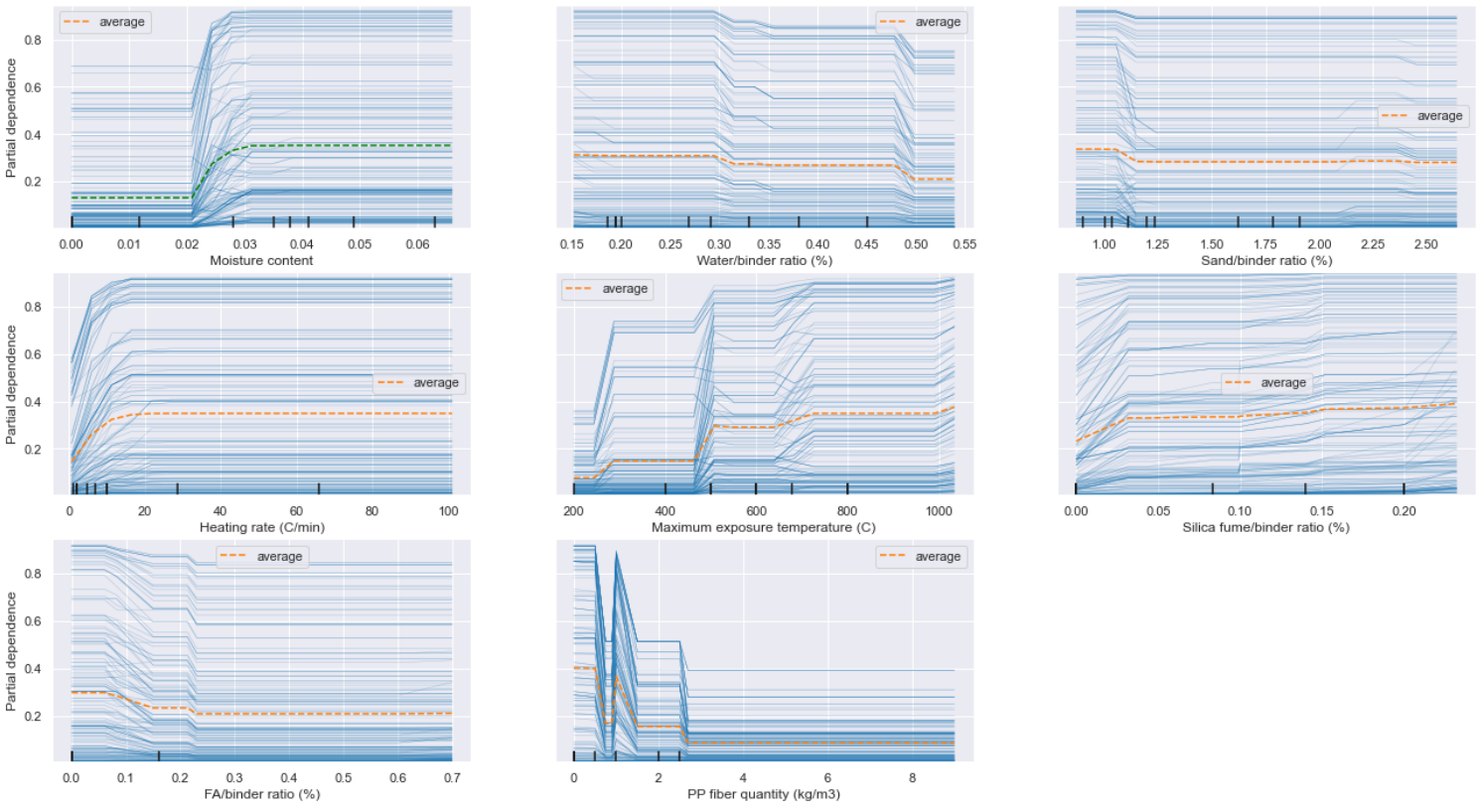

This is a preprint draft. The published article can be found at: https://doi.org/10.1016/j.conbuildmat.2022.128648.

Please cite this paper as:

Al-Bashiti, M., Naser, M.Z. (2022). Verifying Domain Knowledge and Theories on Fire-induced Spalling of Concrete through eXplainable Artificial Intelligence. *Construction and Building Materials*. https://doi.org/10.1016/j.conbuildmat.2022.128648.

Appendix B

This section compares SHAP and LIME predictions for four random specimens A-F.

Specimen A [No Spalling]

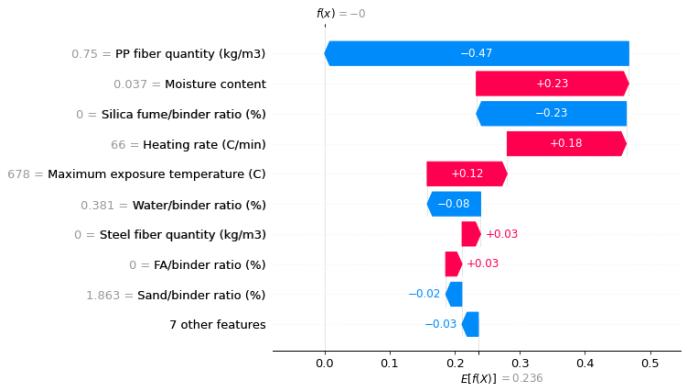

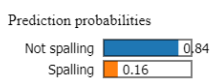

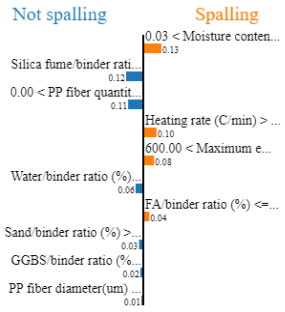

Feature	Value
Moisture content	0.04
Silica fume/binder ratio (%)	0.00
PP fiber quantity (kg/m3)	0.75
Heating rate (C/min)	66.00
Maximum exposure temperature (C)	678.00
Water/binder ratio (%)	0.38
FA/binder ratio (%)	0.00
Sand/binder ratio (%)	1.86
GGBS/binder ratio (%)	0.00
PP fiber diameter(um)	32.00

Specimen B [Spalling]

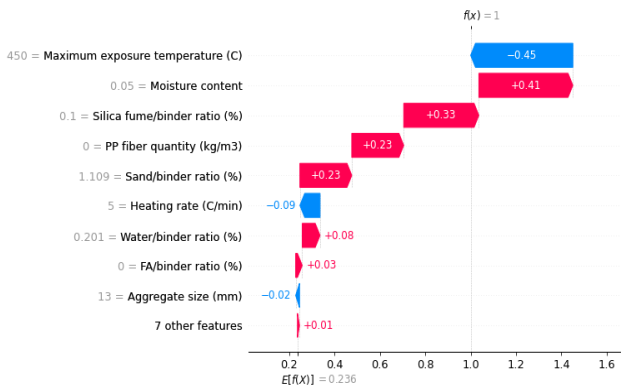

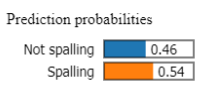

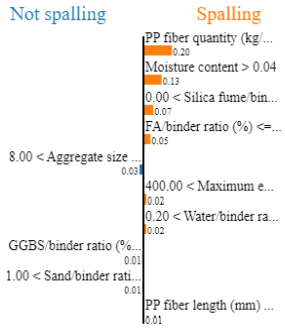

Feature	Value
PP fiber quantity (kg/m3)	0.00
Moisture content	0.05
Silica fume/binder ratio (%)	0.10
FA/binder ratio (%)	0.00
Aggregate size (mm)	13.00
Maximum exposure temperature (C)	450.00
Water/binder ratio (%)	0.20
GGBS/binder ratio (%)	0.00
Sand/binder ratio (%)	1.11
PP fiber length (mm)	0.00

Specimen C [Spalling]

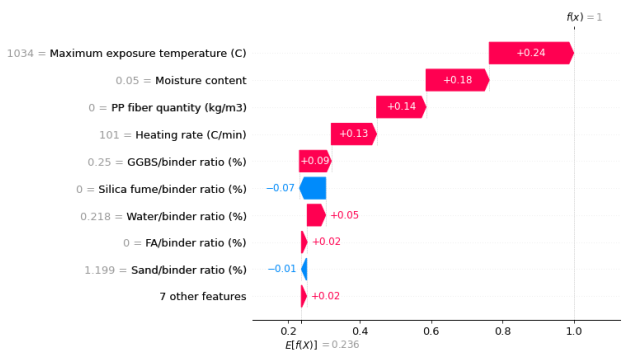

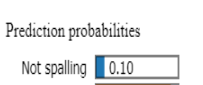

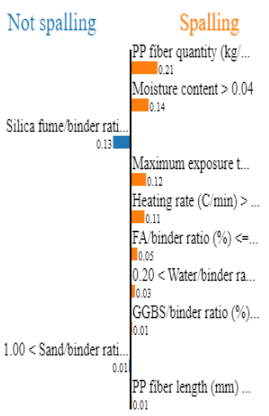

Feature	Value
PP fiber quantity (kg/m3)	0.00
Moisture content	0.05
Silica fume/binder ratio (%)	0.00
Maximum exposure temperature (C)	1034.00
Heating rate (C/min)	101.00
FA/binder ratio (%)	0.00
Water/binder ratio (%)	0.22
GGBS/binder ratio (%)	0.25
Sand/binder ratio (%)	1.20
PP fiber length (mm)	0.00

This is a preprint draft. The published article can be found at: https://doi.org/10.1016/j.conbuildmat.2022.128648.

Please cite this paper as:

Al-Bashiti, M., Naser, M.Z. (2022). Verifying Domain Knowledge and Theories on Fire-induced Spalling of Concrete through eXplainable Artificial Intelligence. *Construction and Building Materials*. https://doi.org/10.1016/j.conbuildmat.2022.128648.

References

[1] R. Jansson, L. Boström, Factors influencing fire spalling of self compacting concrete, Materials and Structures/Materiaux et Constructions. 46 (2013). https://doi.org/10.1617/s11527-012-0007-z.

[2] G.A. Khoury, Effect of fire on concrete and concrete structures, Progress in Structural Engineering and Materials. 2 (2000) 429–447. https://doi.org/10.1002/pse.51.

[3] E.U. Khan, R.A. Khushnood, W.L. Baloch, Spalling sensitivity and mechanical response of an ecofriendly sawdust high strength concrete at elevated temperatures, Construction and Building Materials. 258 (2020). https://doi.org/10.1016/j.conbuildmat.2020.119656.

[4] H.W. Ye, N.Q. Feng, Y. Ling-Hu, Z.W. Ran, L.X. Lin, S.K. Qi, Y. Dong, Research on fire resistance of ultra-high-performance concrete, Advances in Materials Science and Engineering. 2012 (2012). https://doi.org/10.1155/2012/530948.

[5] J.C. Liu, K.H. Tan, Y. Yao, A new perspective on nature of fire-induced spalling in concrete, Construction and Building Materials. 184 (2018). https://doi.org/10.1016/j.conbuildmat.2018.06.204.

[6] R. Jansson, Fire spalling of concrete - A historical overview, in: MATEC Web of Conferences, 2013. https://doi.org/10.1051/matecconf/20130601001.

[7] American Institute of Architects., Society of Fire Protection Engineers., International Code Council., H. International Conference on Performance-Based Codes and Fire Safety Design Methods (2nd : 1998 : Maui, Proceedings : 1998 Pacific Rim Conference and second International Conference on Performance-based Codes and Fire Safety Design Methods, May 3-9, 1998, Maui, Hawaii, (n.d.) 620.

[8] The effect of fire - Concrete spalling - Promat, (n.d.). https://www.promat.com/en/tunnels/your-project/expert-area/159998/the-effect-of-fire-concrete-spalling/ (accessed April 14, 2022).

[9] P. Lura, G. pietro Terrasi, Reduction of fire spalling in high-performance concrete by means of superabsorbent polymers and polypropylene fibers: Small scale fire tests of carbon fiber reinforced plastic-prestressed self-compacting concrete, Cement and Concrete Composites. 49 (2014). https://doi.org/10.1016/j.cemconcomp.2014.02.001.

[10] R. Jansson, Fire Spalling of Concrete: Theoretical and Experimental Studies, Cement and Concrete Composites. 26 (2013).

[11] K.D. Hertz, Limits of spalling of fire-exposed concrete, Fire Safety Journal. 38 (2003). https://doi.org/10.1016/S0379-7112(02)00051-6.

[12] J.C. Liu, K.H. Tan, Fire resistance of strain hardening cementitious composite with hybrid PVA and steel fibers, Construction and Building Materials. 135 (2017). https://doi.org/10.1016/j.conbuildmat.2016.12.204.

[13] E.W.H. Klingsch, Explosive spalling of concrete in fire, ETH Union. (2014).

[14] L.T. Phan, J.R. Lawson, F.L. Davis, Effects of elevated temperature exposure on heating characteristics, spalling, and residual properties of high performance concrete, Materials and Structures/Materiaux et Constructions. 34 (2001). https://doi.org/10.1007/bf02481556.

[15] K. Hertz, Explosion of silica-fume concrete, Fire Safety Journal. 8 (1984). https://doi.org/10.1016/0379-7112(84)90057-2.

[16] A.N. Noumowe, P. Clastres, G. Debicki, J.L. Costaz, Transient heating effect on high strength concrete, Nuclear Engineering and Design. 166 (1996). https://doi.org/10.1016/0029-5493(96)01235-6.

[17] Effect of transient high temperature on high-strength concrete - ProQuest, (n.d.). https://www.proquest.com/docview/193775368?pq-origsite=gscholar&fromopenview=true (accessed April 14, 2022).

[18] M.Z. Naser, V.K. Kodur, Explainable machine learning using real, synthetic and augmented fire tests to predict fire resistance and spalling of RC columns, Engineering Structures. 253 (2022) 113824. https://doi.org/10.1016/J.ENGSTRUCT.2021.113824.

[19] L.T. Phan, Pore pressure and explosive spalling in concrete, Materials and Structures/Materiaux et Constructions. 41 (2008). https://doi.org/10.1617/s11527-008-9353-2.

[20] C.G. Han, Y.S. Hwang, S.H. Yang, N. Gowripalan, Performance of spalling resistance of high performance concrete with polypropylene fiber contents and lateral confinement, Cement and Concrete Research. 35 (2005). https://doi.org/10.1016/j.cemconres.2004.11.013.

[21] F. lo Monte, R. Felicetti, Spalling sensitivity test on concrete, Lecture Notes in Civil Engineering. 10 (2016) 512–523. https://doi.org/10.1007/978-3-319-78936-1_37.

[22] M.Z. Naser, Mechanistically Informed Machine Learning and Artificial Intelligence in Fire Engineering and Sciences, Fire Technology 2021 57:6. 57 (2021) 2741–2784. https://doi.org/10.1007/S10694-020-01069-8.

[23] C. Rudin, Stop explaining black box machine learning models for high stakes decisions and use interpretable models instead, Nature Machine Intelligence. 1 (2019). https://doi.org/10.1038/s42256-019-0048-x.

[24] M.Z. Naser, An engineer's guide to eXplainable Artificial Intelligence and Interpretable Machine Learning: Navigating causality, forced goodness, and the false perception of inference, Automation in Construction. 129 (2021) 103821. https://doi.org/10.1016/J.AUTCON.2021.103821.

[25] C. Rudin, J. Radin, Why Are We Using Black Box Models in AI When We Don't Need To? A Lesson From An Explainable AI Competition, Harvard Data Science Review. 1 (2019). https://doi.org/10.1162/99608f92.5a8a3a3d.

[26] M.Z. Naser, An engineer's guide to eXplainable Artificial Intelligence and Interpretable Machine Learning: Navigating causality, forced goodness, and the false perception of inference, Automation in Construction. 129 (2021). https://doi.org/10.1016/j.autcon.2021.103821.

[27] The construction industry's productivity problem | The Economist, (n.d.). https://www.economist.com/leaders/2017/08/17/the-construction-industrys-productivity-problem (accessed April 14, 2022).

[28] R. Bogue, What are the prospects for robots in the construction industry?, Industrial Robot. 45 (2018). https://doi.org/10.1108/IR-11-2017-0194.

[29] Gary, M., Brandproben an Eisenbetongbasuten (in German), Deutcher Ausschlutss für Eisenbetong, Heft 41, Berlin, Germany, 1918., (n.d.).

[30] Gary, M., Brandproben an Eisenbetongbasuten (in German), Deutcher Ausschlutss für Eisenbetong, Heft 33, Berlin, Germany, 1916., (n.d.).

[31] Gary, M., Brandproben an Eisenbetongbasuten (in German), Deutcher Ausschlutss für Eisenbetong, Heft 11, Berlin, Germany, 1911., (n.d.).

[32] C. Meyer-Ottens, Zur Frage der Abplatzungen an Betonbauteilen aus Normalbeton bei Brandbeanspruchung, (1972). https://doi.org/10.24355/DBBS.084-201503301029-0.

[33] I. Hager, K. Mróz, Role of Polypropylene Fibres in Concrete Spalling Risk Mitigation in Fire and Test Methods of Fibres Effectiveness Evaluation, Materials. 12 (2019). https://doi.org/10.3390/ma12233869.

[34] E. Hwang, G. Kim, G. Choe, M. Yoon, M. Son, D. Suh, H. Eu, J. Nam, Explosive Spalling Behavior of Single-Sided Heated Concrete According to Compressive Strength and Heating Rate, Materials. 14 (2021). https://doi.org/10.3390/MA14206023.

[35] The influence of stress-strain conditions on fire-induced concrete spalling: A review - UQ eSpace, (n.d.). https://espace.library.uq.edu.au/view/UQ:3748a42 (accessed May 19, 2022).

[36] Hasenjäger, Über das Verhalten des Betons und Eisenbetons im Feuer und die Ausbildung von Dehnungsfugen im Eisenbetonbau, Dissertation, Techniche Hochschole Braunschweig,as cited by: Meyer-Ottens C., Zur Frage der Abplatzungen an Betonbauteilen aus Normalbeton bei Brandbeanspruchung, PhD-thesis , (n.d.).

[37] K.D. Hertz, Limits of spalling of fire-exposed concrete, Fire Safety Journal. 38 (2003) 103–116. https://doi.org/10.1016/S0379-7112(02)00051-6.

[38] V.K.R. Kodur, Spalling in High Strength Concrete Exposed to Fire: Concerns, Causes, Critical Parameters and Cures, Structures Congress 2000: Advanced Technology in Structural Engineering. 103 (2004) 1–9. https://doi.org/10.1061/40492(2000)180.

[39] W.J. Copier, The Spalling of Normal Weight and Lightweight Concrete Exposed to Fire, (n.d.). https://www.concrete.org/publications/internationalconcreteabstractsportal/m/details/id/6591 (accessed April 14, 2022).

[40] J. Ko, D. Ryu, T. Noguchi, The spalling mechanism of high-strength concrete under fire, Magazine of Concrete Research. 63 (2011). https://doi.org/10.1680/macr.10.00002.

[41] S.Y.N. Chan, G.F. Peng, M. Anson, Fire behavior of high-performance concrete made with silica fume at various moisture contents, ACI Materials Journal. 96 (1999). https://doi.org/10.14359/640.

[42] C. Meyer-Ottens, The Question of Spalling of Concrete... - Google Scholar, (n.d.). https://scholar.google.com/scholar?hl=en&as_sdt=0%2C41&q=C.+Meyer-Ottens%2C+The+Question+of+Spalling+of+Concrete+Structural+Elements+of+Standard+Concrete+Under+Fire+Loading&btnG= (accessed April 14, 2022).

[43] Klingsch, Eike. “Explosive spalling of concrete in fire.” (2014)., (n.d.).

[44] EN 1992-1-2: Eurocode 2: Design of concrete structures - Part 1-2: General rules - Structural fire design, (1992).

[45] M.B. Dwaikat, V.K.R. Kodur, Fire induced spalling in high strength concrete beams, Fire Technology. 46 (2010). https://doi.org/10.1007/s10694-009-0088-6.

[46] T.Z. Harmathy, Effect of Moisture on the Fire Endurance of Building Elements, in: Moisture in Materials in Relation to Fire Tests, 2009. https://doi.org/10.1520/stp48429s.

[47] (PDF) Experimental study on the contribution of pore vapour pressure to the thermal instability risk of concrete. Concrete spalling due to fire exposure | Pierre Pimienta - Academia.edu, (n.d.). https://www.academia.edu/18040159/Experimental_study_on_the_contribution_of_pore_vapour_pressure_to_the_thermal_instability_risk_of_concrete_Concrete_spalling_due_to_fire_exposure (accessed April 14, 2022).

[48] M.B. Dwaikat, V.K.R. Kodur, Hydrothermal model for predicting fire-induced spalling in concrete structural systems, Fire Safety Journal. 44 (2009). https://doi.org/10.1016/j.firesaf.2008.09.001.

[49] Y. Ichikawa, G.L. England, Prediction of moisture migration and pore pressure build-up in concrete at high temperatures, in: Nuclear Engineering and Design, 2004. https://doi.org/10.1016/j.nucengdes.2003.06.011.

[50] M. Ozawa, H. Morimoto, Effects of various fibres on high-temperature spalling in high-performance concrete, Construction and Building Materials. 71 (2014). https://doi.org/10.1016/j.conbuildmat.2014.07.068.

[51] Harmathy TZ. Effect of Moisture on the Fire Endurance of Building Elements. Research Paper 270, Division of Building Research. Ottawa 1965. Or: Moisture in Materials in relation to Fire Tests. ASTM, Special Technical Publication No. 385,1964;74–95., (n.d.).

[52] \YKOB, B.B.: &pn#hFi bzpFiboodpazholo pazpyvehnr detoha fpn fo|ae.]etoh n |ejezodetoh 3:1976. pp. 26–28. (Zhukov VV.: Reasons for explosive deterioration of concrete during fire. In Russian. Concrete and Reinforced Concrete 1976;3:26–8.), (n.d.).

[53] Barret, On the French and other methods of constructing iron floors, Civil Engineering and Architect's Journal, Vol XVII, pp 94,1854, (n.d.).

[54] K. Hertz, Explosion of silica-fume concrete, Fire Safety Journal. 8 (1984) 77. https://doi.org/10.1016/0379-7112(84)90057-2.

[55] ACI CODE-318-14: Building Code Requirements for Structural Concrete and Commentary, (n.d.). https://www.concrete.org/store/productdetail.aspx?ItemID=318U14&Language=English&Units=US_Units (accessed April 25, 2022).

[56] G.A. Khoury, Polypropylene fibres in heated concrete. Part 2: Pressure relief mechanisms and modelling criteria, Magazine of Concrete Research. 60 (2008). https://doi.org/10.1680/macr.2007.00042.

[57] A. Bilodeau, V.K.R. Kodur, G.C. Hoff, Optimization of the type and amount of polypropylene fibres for preventing the spalling of lightweight concrete subjected to hydrocarbon fire, Cement and Concrete Composites. 26 (2004). https://doi.org/10.1016/S0958-9465(03)00085-4.

[58] K.K. Sideris, P. Manita, Residual mechanical characteristics and spalling resistance of fiber reinforced self-compacting concretes exposed to elevated temperatures, Construction and Building Materials. 41 (2013). https://doi.org/10.1016/j.conbuildmat.2012.11.093.

[59] Y. Ding, C. Zhang, M. Cao, Y. Zhang, C. Azevedo, Influence of different fibers on the change of pore pressure of self-consolidating concrete exposed to fire, Construction and Building Materials. 113 (2016). https://doi.org/10.1016/j.conbuildmat.2016.03.070.

[60] V.R.; Kodur, M.A. Sultan, Structural behaviour of high strength concrete columns exposed to fire, International Symposium on High Performance and Reactive Powder Concrete. (1998).

[61] Marine concrete structures exposed to hydrocarbon... - Google Scholar, (n.d.). https://scholar.google.com/scholar?hl=en&as_sdt=0%2C41&q=Marine+concrete+structures+exposed+to+hydrocarbon+fires%2C+Report%2C+SINTEF%E2%80%94The+Norwegian+Fire+Research+I&btnG= (accessed April 14, 2022).

[62] J.C. Liu, L. Huang, Z. Tian, H. Ye, Knowledge-enhanced data-driven models for quantifying the effectiveness of PP fibers in spalling prevention of ultra-high performance concrete, Construction and Building Materials. 299 (2021) 123946. https://doi.org/10.1016/J.CONBUILDMAT.2021.123946.

[63] J.C. Liu, L. Huang, Z. Chen, H. Ye, A comparative study of artificial intelligent methods for explosive spalling diagnosis of hybrid fiber-reinforced ultra-high-performance concrete, International Journal of Civil Engineering. (2021) 1–22. https://doi.org/10.1007/S40999-021-00689-7/FIGURES/19.

[64] J.C. Liu, Z. Zhang, A machine learning approach to predict explosive spalling of heated concrete, Archives of Civil and Mechanical Engineering. 20 (2020) 1–25. https://doi.org/10.1007/S43452-020-00135-W/TABLES/10.

[65] J.C. Liu, Z. Zhang, Neural network models to predict explosive spalling of PP fiber reinforced concrete under heating, Journal of Building Engineering. 32 (2020) 101472. https://doi.org/10.1016/J.JOBE.2020.101472.

[66] J.C. Liu, Z. Zhang, Prediction of Explosive Spalling of Heated Steel Fiber Reinforced Concrete using Artificial Neural Networks, Journal of Advanced Concrete Technology. 18 (2020) 227–240. https://doi.org/10.3151/JACT.18.227.

[67] M.Z. Naser, V. Kodur, H.T. Thai, R. Hawileh, J. Abdalla, V. v. Degtyarev, StructuresNet and FireNet: Benchmarking databases and machine learning algorithms in structural and fire engineering domains, Journal of Building Engineering. 44 (2021) 102977. https://doi.org/10.1016/J.JOBE.2021.102977.

[68] T. Chen, C. Guestrin, XGBoost: A Scalable Tree Boosting System, Proceedings of the 22nd ACM SIGKDD International Conference on Knowledge Discovery and Data Mining. (n.d.). https://doi.org/10.1145/2939672.

[69] A Unified Approach to Interpreting Model Predictions, (n.d.). https://proceedings.neurips.cc/paper/2017/hash/8a20a8621978632d76c43dfd28b67767-Abstract.html (accessed April 14, 2022).

[70] L.S. Shapley, 17. A Value for n-Person Games, Contributions to the Theory of Games (AM-28), Volume II. (2016) 307–318. https://doi.org/10.1515/9781400881970-018.

[71] M.T. Ribeiro, S. Singh, C. Guestrin, "Why Should I Trust You?" Explaining the Predictions of Any Classifier, Proceedings of the 22nd ACM SIGKDD International Conference on Knowledge Discovery and Data Mining. (n.d.). https://doi.org/10.1145/2939672.

[72] V.K.R. Kodur, L. Phan, Critical factors governing the fire performance of high strength concrete systems, Fire Safety Journal. 42 (2007) 482–488. https://doi.org/10.1016/J.FIRESAF.2006.10.006.

[73] G. Choe, G. Kim, M. Yoon, E. Hwang, … J.N.-C. and C., undefined 2019, Effect of moisture migration and water vapor pressure build-up with the heating rate on concrete spalling type, Elsevier. (n.d.). https://www.sciencedirect.com/science/article/pii/S0008884617309493 (accessed May 13, 2022).